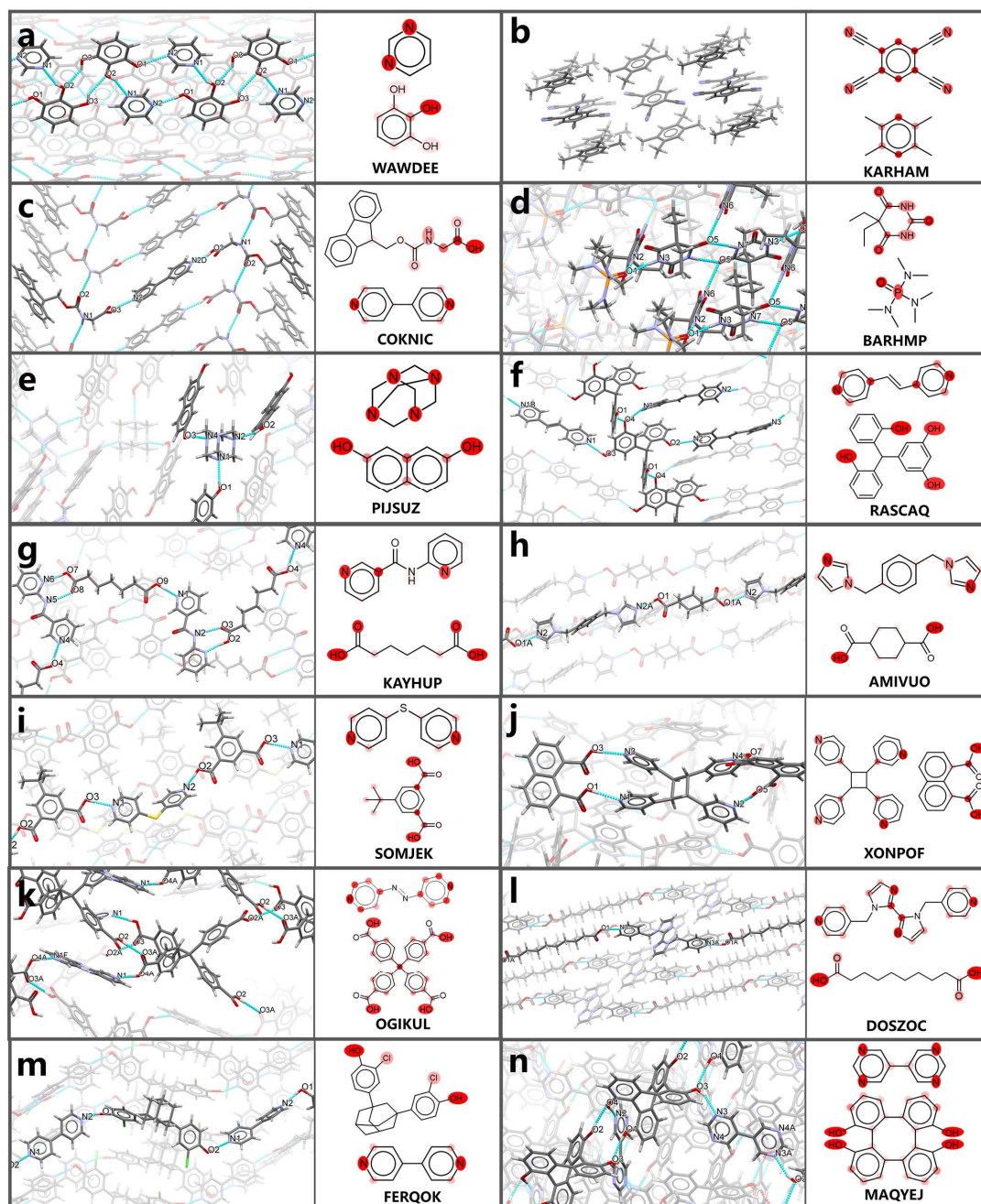


**Supplementary Information**

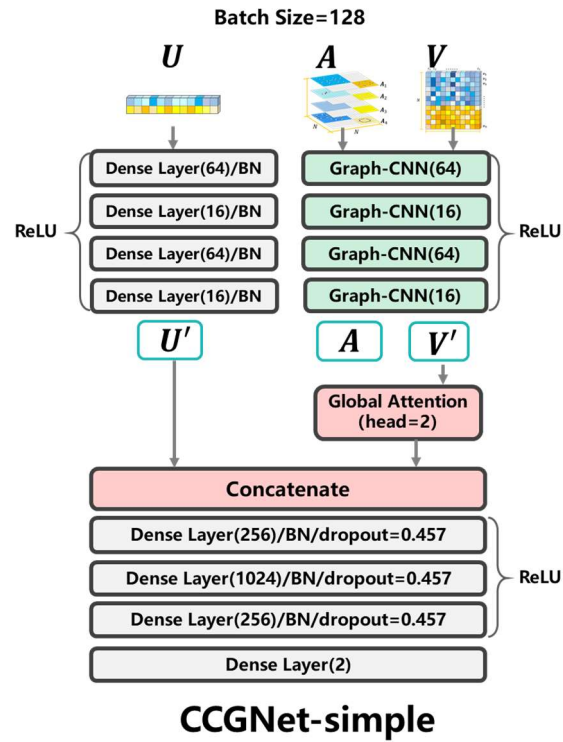
**Coupling Complementary Strategy to Flexible Graph  
Neural Network for Quick Discovery of Coformer in  
Diverse Co-crystal Materials**

Y. Jiang et al.

## Supplementary Figures

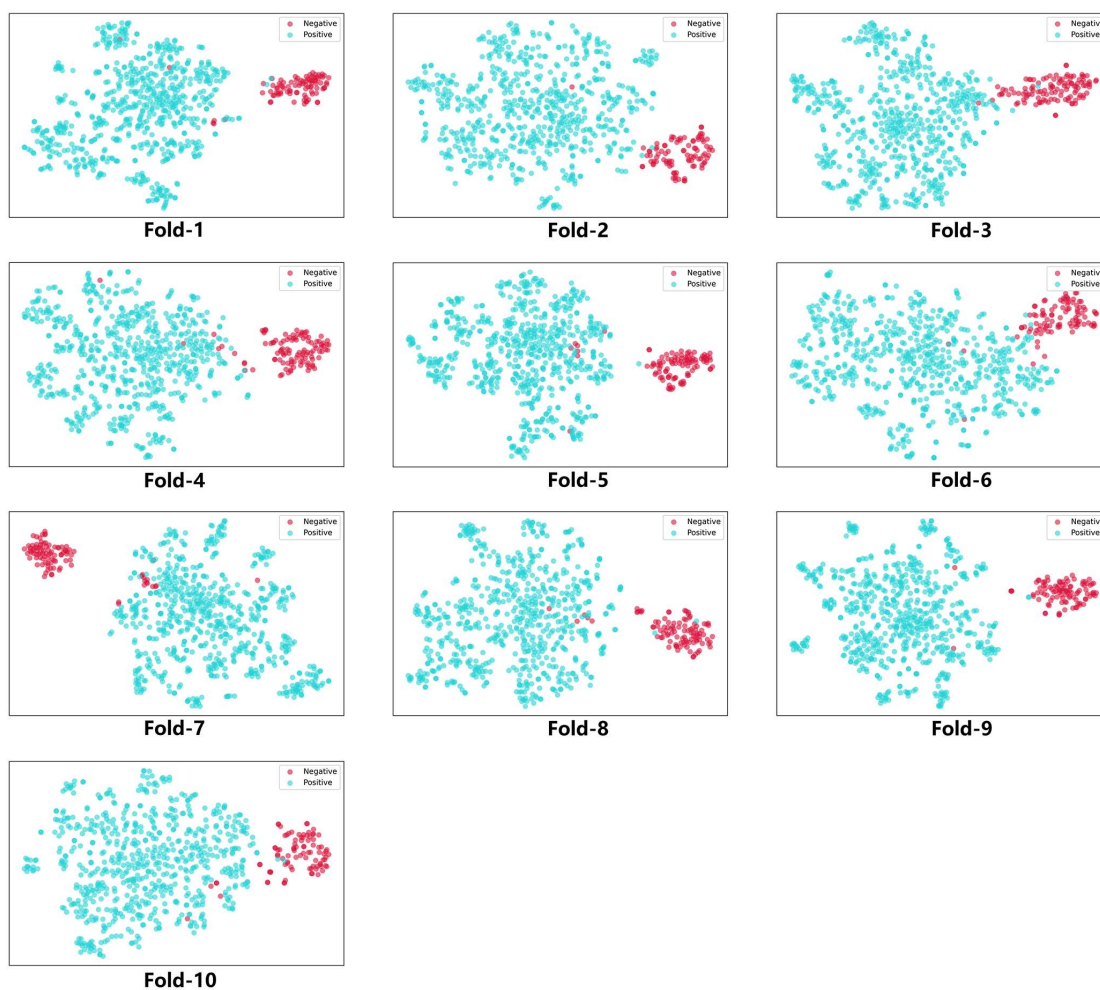


**Supplementary Figure 1:** Attention visualization for some representative cocrystals. **a** WAWDEE. **b** KARHAM. **c** COKNIC. **d** BARHMP. **e** PIJSUZ. **f** RASCAQ. **g** KAYHUP. **h** AMIVUO. **i** SOMJEK. **j** XONPOF. **k** OGIKUL. **l** DOSZOC. **m** FERQOK. **n** MAQYEJ. The real cocrystal structure is displayed by Mercury while the corresponding 2D structure is highlighted by the attention weights derived from CCGNet. The redder the color, the greater the attention weight. The cyan dash line denotes the intermolecular H-bonding.



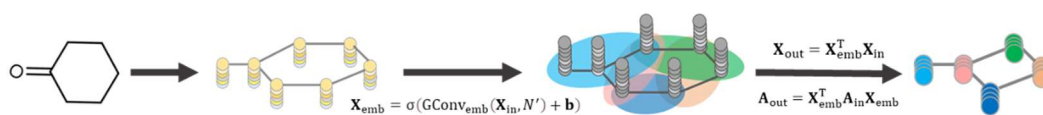
**Supplementary Figure 2:** Configuration of CCGNet-simple.

The concatenation operation between the node feature and the global state in each CCGBlock is removed, only retaining the concatenation at the readout stage.

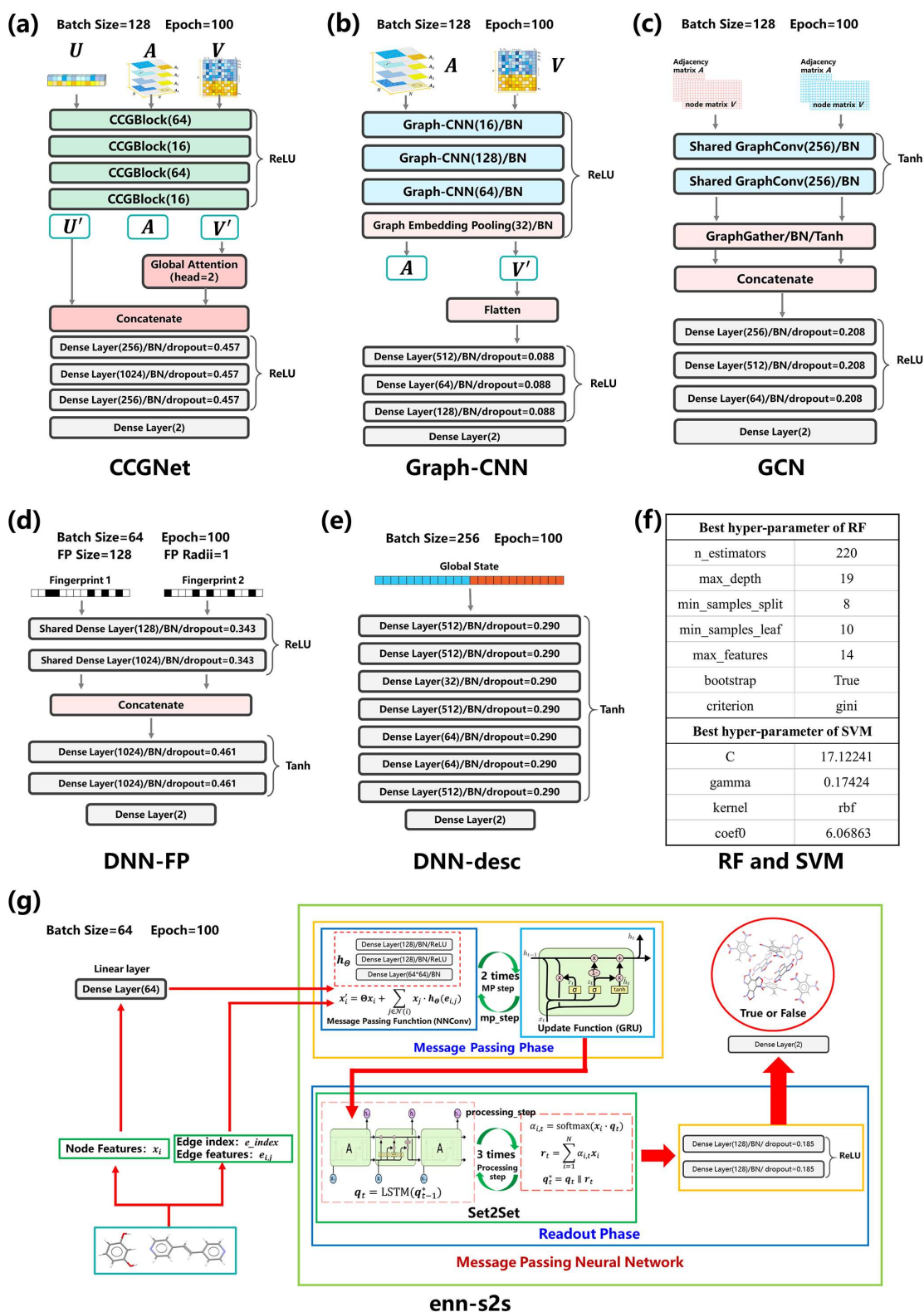


**Supplementary Figure 3:** t-SNE analysis on each fold of the 10-fold cross-validation for CCGNet.

Hidden representations are extracted after the concatenation operation of the readout phase. Blue dot: positive sample. Red dot: negative sample.

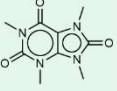
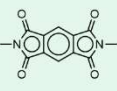
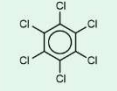
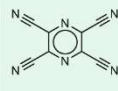
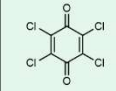
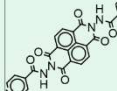
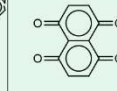
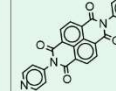
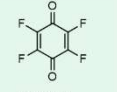
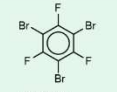
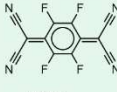
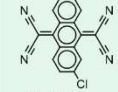
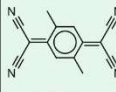
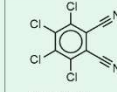
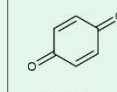
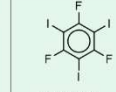

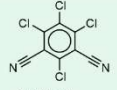
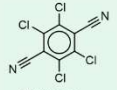
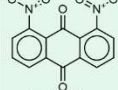
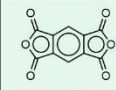
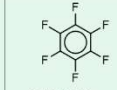
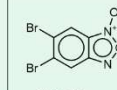
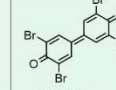
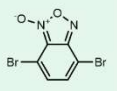
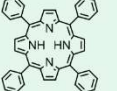
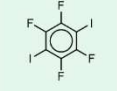
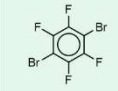
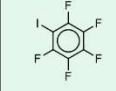
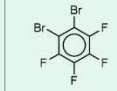
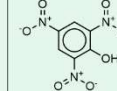
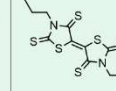
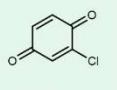
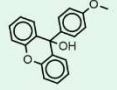
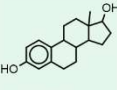
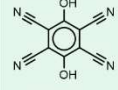
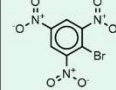
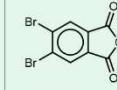
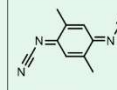
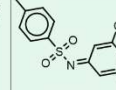
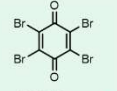
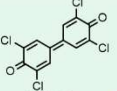
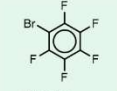
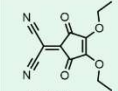
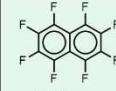
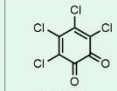
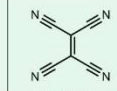
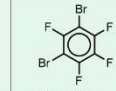
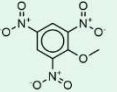
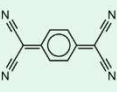
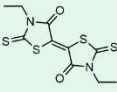
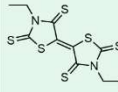

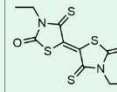
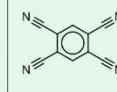
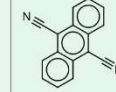
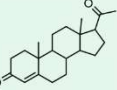
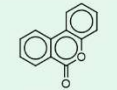
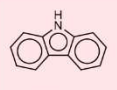
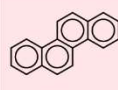
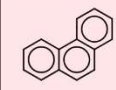
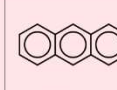




**Supplementary Figure 4:** The process of Graph Embed Pooling.



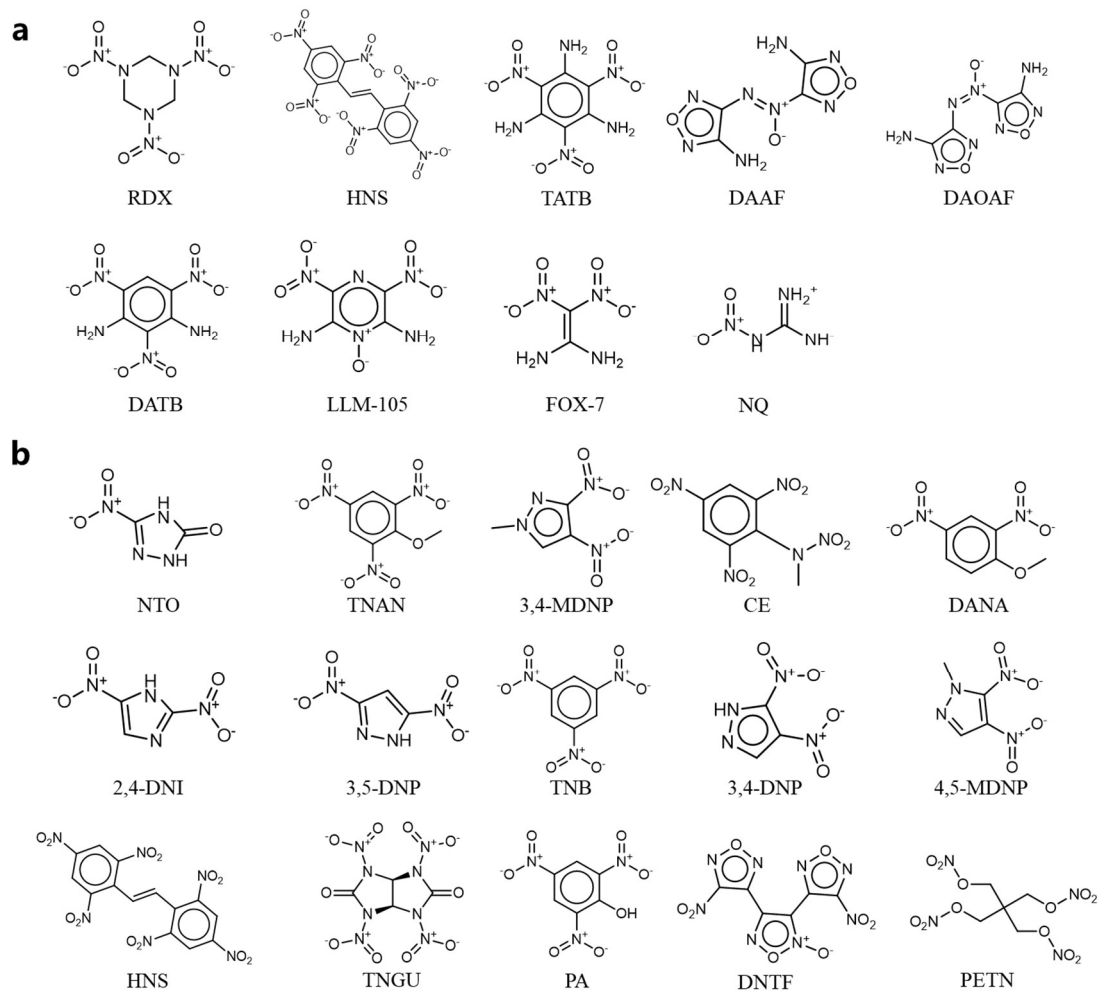
**Supplementary Figure 5:** The best configurations of all the models, derived from the optimized hyper-parameters.

(a) CCGNet. (b) Graph-CNN. (c) GCN. (d) DNN-FP. (e) DNN-desc. (f) RF and SVM. (g) enn-s2s.

 MURPYR Score: 51.82 ✓	 PAYYOG Score: 50.68 ✓	 ISISAG Score: 50.12 ✓	 BORPII Score: 49.93 ✓	 PYRCLN Score: 49.61 ✓	 OPUQUN Score: 48.98 ✓	 CEKBUP Score: 48.75 ✓	 GUMNUY Score: 48.65 ✓
 PYRFLR Score: 48.84 ✓	 QEVXOH Score: 48.62 ✓	 MIDDLEL Score: 48.37 ✓	 GAFJAY Score: 48.36 ✓	 VOQCUC Score: 48.12 ✓	 PINJU02 Score: 47.83 ✓	 PYRBZQ Score: 47.63 ✓	 QEVWEW Score: 47.46 ✓
 CUNWUD Score: 47.42 ✓	 HAYYOW Score: 47.39 ✓	 WAWPAM Score: 47.37 ✓	 AGORAS Score: 47.29 ✓	 PYRPA01 Score: 47.27 ✓	 ZZZGKE01 Score: 47.24 ✓	 EHESIT Score: 47.21 ✓	 BAZCUA Score: 47.13 ✓
 AYEGAM Score: 46.98 ✓	 XAGMAT Score: 46.89 ✓	 FARNOD Score: 46.78 ✓	 GUQRAN Score: 46.77 ✓	 GUQQIU Score: 46.64 ✓	 GUQQQA Score: 46.58 ✓	 PYRPT02 Score: 46.48 ✓	 QQLREQ Score: 46.42 ✓
 CORPIJ Score: 46.41 ✓	 XETTEW Score: 46.38 ✓	 CUTBEZ Score: 46.35 ✓	 TEXPOB Score: 46.20 ✓	 PYRBPC Score: 46.18 ✓	 EHESUF Score: 46.17 ✓	 VOQDAJ Score: 46.14 ✓	 PYTQIM Score: 46.08 ✓
 REDFIP Score: 46.06 ✓	 BAZDAH Score: 46.00 ✓	 GUQEQ Score: 45.97 ✓	 BEFGIC Score: 45.92 ✓	 ECUVIH Score: 45.88 ✓	 REQVOZ Score: 45.87 ✓	 PYRCYE10 Score: 45.86 ✓	 GUQQUG Score: 45.83 ✓
 CILRAQ Score: 45.86 ✓	 BITBUD Score: 45.42 ✓	 QQLQQA Score: 45.01 ✓	 QQLPUF Score: 44.92 ✓	 GUQQAM Score: 44.88 ✓	 QQLRER Score: 44.80 ✓	 PYRCBZ Score: 44.77 ✓	 EHUFEV Score: 44.72 ✓
 CUSZUM Score: 43.43 ✓	 EHUFIZ Score: 10.97 ✓	 6854 Score: -58.21 ✓	 9171 Score: -61.49 ✓	 995 Score: -62.48 ✓	 8418 Score: -63.74 ✓	 931 Score: -64.69 ✓	 9154 Score: -72.37 ✓

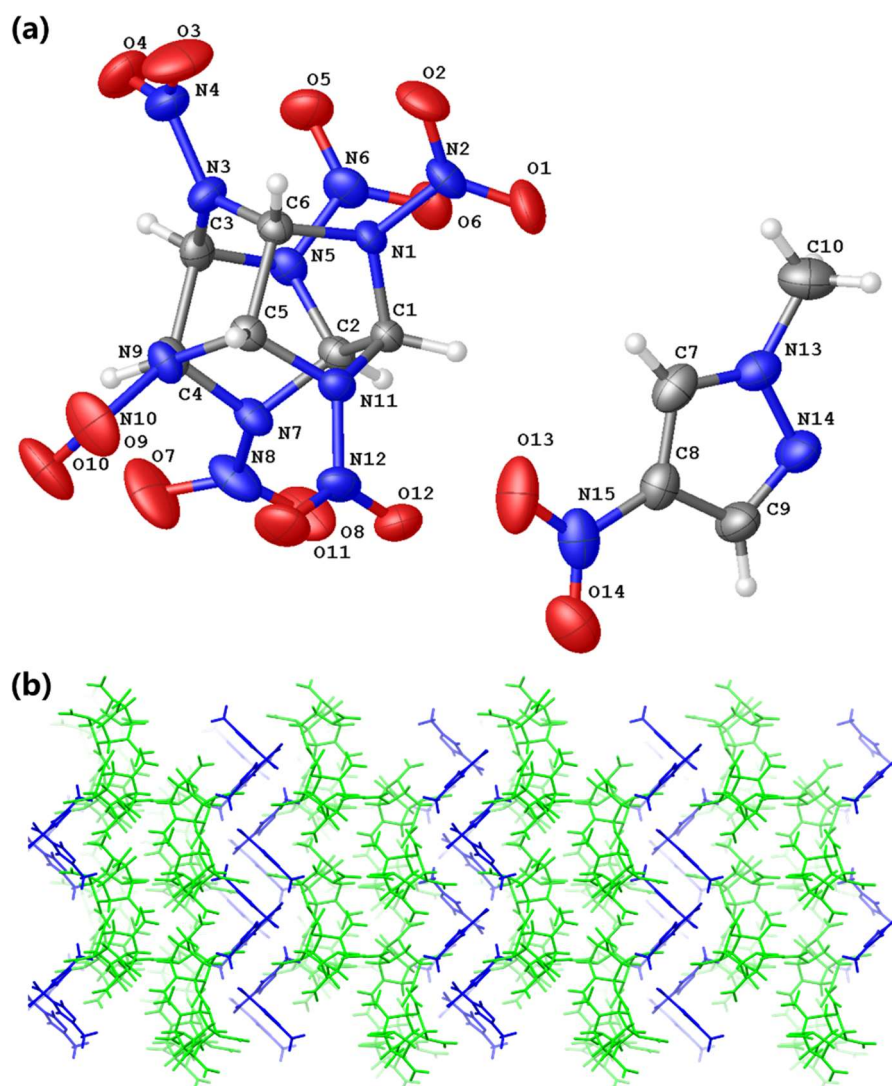
**Supplementary Figure 6:** The predictive score ranking of CCGNet from high to low for the cofomers of Pyrene.

Green background: True Positive sample; red background: True Negative sample. The green tick and red cross denote the correct prediction and the wrong prediction, respectively. The cofomer of the positive sample is labeled as the CSD refcode while the negative sample is named in terms of PubChem Compound ID.



**Supplementary Figure 7:** Molecules used to construct the energetic cocrystal negative samples.

**a** Structures of nine energetic molecules served as cofomers of potential negative samples for the ISPE calculation. **b** Structures of fifteen cofomers derived from failed co-crystallization with CL-20 in our experimental works.



**Supplementary Figure 8:** Crystal structure of CL-20/1-Methyl-4-nitropyrazole.

(a) ORTEP plot of the cocrystal. (b) The molecular arrangement for CL-20 and 1-Methyl-4-nitropyrazole in cocrystal. Green: CL-20. Blue: 1-Methyl-4-nitropyrazole.



## Supplementary Tables

**Supplementary Table 1.** Solvents involved in collecting cocrystal positive samples from CSD.

Toluene	4-Chlorotoluene	diglyme
DMSO-d6	1,3,5-trichlorobenzene	iodobenzene
trichloromethane-d	gamma-Butyrolactone	1,1,2-trichloroethane
ethoxyethane	DL-sec-Butyl acetate	formic acid
methylamine	iodomethane	dimethyl sulfoxide
p-Xylene	methanamide	3-methyl-1-butanol
1-butanol	Tetrahydrofuran	bromobenzene
cyclohexanone	chlorobenzene	dimethoxymethane
1H-pyrrole	Ethyl formate	2-butanone
2-butanol	isobutanol	N-Ethylmorpholine
1,1,2,2-tetrachloroethane	N, N, N', N'-Tetramethylethylenediamine	propan-2-ol
1,4-dioxane	Ethanol	2-methyl-2-propanol
2-methylpyridine	3-methylpyridine	2-butoxyethanol
diethylenetriamine	2-methoxyethanol	dibromomethane
1-methyl-2-pyrrolidone	N, N-dimethylacetamide	2,2'-Dichlorodiethyl ether
Methyl acetate	cyclopentane	benzyl alcohol
benzene	hexadecane	water-d2
nitromethane	hexamethyldisiloxane	Hexane
1-Chloro-2-Methylpropane	acetic anhydride	propanenitrile
acetamide	acetic acid	Ethylene glycol
Diethylene glycol	Isopropyl acetate	Isopropyl ether
tetrachloromethane	acetone	acetophenone
nitrobenzene	propionic acid	1,2-Propanediol
pentane	1,1-Dichloroethane	butane-1,4-diol
1,3-dimethylbenzene	1,2-dihydrostilbene	N, N-diethylethanamine
tribromomethane	2-propoxyethanol	1,2-Dichloroethane
1-propanol	water	phenylamine
heptane	trichloromethane	pyridine
cyclohexene	cyclohexane	Methanol
1,2-dimethoxyethane	3-pentanone	fluorobenzene
epichlorohydrin	acetonitrile	dichloromethane
methanedithione	1-Octanol	butanedioic acid
N, N-dimethylformamide	1,2-ethanediamine	2,4-pentanedione
o-Xylene	Propylene glycol monomethyl ether acetate	1,3,5-trimethylbenzene
2-phenylacetonitrile	2-Chlorotoluene	1,2-dichlorobenzene
isophorone	morpholine	nitric acid
quinoline	benzonitrile	ethyl acetate
benzene-d6		

**Supplementary Table 2.** Search spaces of hyper-parameters for CCGNet, Graph-CNN and enn-s2s.

	CCGNet		Graph-CNN		enn-s2s	
<b>Training</b>	Batch size	128	Batch size	128	Batch size	32
	Epoch	100	Epoch	100	Epoch	100
	Optimizer	Adam	Optimizer	Adam	Optimizer	Adam
<b>Message Passing (MP) Phase</b>	Number of CCGBlock	1,2,3,4,5,6,	Number of Graph-CNN layer	1,2,3	Linear layer size	32,64,128
			Size of Graph-CNN layer	16,32,64,128,256	Number of dense layers in $h_{\theta}$	1,2,3
	CCGBlock Size	16,32,64,128,256	Number of Graph embedding pooling	1,2,3	Size of dense layer in $h_{\theta}$ (not out layer)	128,512,1024,2048
					Size of output layer in $h_{\theta}$	(Linear layer size) <sup>2</sup>
			Size of Graph embedding pooling	8,16,32	MP step	2,3,4,5
	Activation function	ReLU, ELU, Tanh	Activation function	ReLU	Activation function	ReLU
<b>Readout Phase</b>	Readout function	Multi-head global attention	Readout function	Flatten	Readout function	Set2Set
	Number of head	Integer, [1, 20]			Processing step	2,3,4,5
	Number of dense layers	1,2,3	Number of dense layers	1,2,3	Number of dense layers	1,2,3
	Dense layer size	64,128,256,512,1024	Dense layer size	64,128,256,512	Dense layer size	64,128,256,512,1024
	Dropout	float, [0, 0.75]	Dropout	float, [0, 0.75]	Dropout	float, [0, 0.75]
	Activation function	ReLU, ELU, Tanh	Activation function	ReLU	Activation function	ReLU
<b>Output</b>	Dense layer size	2	Dense layer size	2	Dense layer size	2

**Supplementary Table 3.** Search spaces of hyper-parameters for RF, SVM and DNN-desc.

RF		SVM		DNN-desc	
<b>Number of estimators</b>	int, [10, 500], step=10	<b>C</b>	float, [0, 20]	<b>Batch size</b>	64,128,256
				<b>Epoch</b>	100
				<b>Optimizer</b>	Adam
<b>Max depth</b>	int, [1, 20]	<b>degree</b>	int, [1, 20]	<b>Number of dense layers</b>	1,2,3,4,5,6,7
<b>Min samples split</b>	int, [2, 200]	<b>gamma</b>	float or string, {[0, 1], scale, auto}	<b>Size of dense layer</b>	16,32,64,128,256,512
<b>Min samples leaf</b>	int, [1, 50]			<b>dropout</b>	float, [0, 0.75]
<b>Max features</b>	int, [1, 24]	<b>coef0</b>	float, [0, 10]	<b>Activation function</b>	ReLU, ELU, Tanh
<b>Criterion</b>	string, {gini, entropy}	<b>kernel</b>	String, {rbf, poly, sigmoid, linear}	<b>Output size</b>	2
<b>Bootstrap</b>	bool {True, False}				

**Supplementary Table 4.** The performances of all the models on the 10-fold cross-validation with and without the data augmentation. ‘c1-c2’ and ‘c2-c1’ denote two different permutations in the model input for a pair of cofomers.

Model	Metrics	Data Augmentation <sup>a</sup>		No Data Augmentation <sup>b</sup>	
		c1-c2	c2-c1	c1-c2	c2-c1
SVM	TPR	99.11(±0.41)	99.11(±0.41)	99.17(±0.27)	98.51(±0.40)
	TNR	89.81(±3.55)	89.81(±3.55)	88.54(±2.52)	61.03(±4.58)
	BACC	94.46(±1.85)	94.46(±1.85)	93.85(±1.34)	79.77(±2.27)
RF	TPR	99.82(±0.15)	99.85(±0.17)	99.88(±0.11)	99.73(±0.20)
	TNR	87.05(±3.87)	86.43(±3.59)	86.05(±3.48)	72.36(±3.77)
	BACC	93.44(±1.89)	93.14(±1.75)	92.97(±1.71)	86.04(±1.87)
DNN-desc	TPR	99.55(±0.19)	99.21(±0.26)	99.59(±0.41)	98.36(±0.99)
	TNR	89.11(±2.42)	89.80(±2.95)	89.66(±4.13)	65.16(±5.49)
	BACC	94.33(±1.25)	94.51(±1.51)	94.62(±1.91)	81.76(±2.48)
DNN-FP	TPR	98.57(±0.46)	98.51(±0.32)	99.17(±0.35)	97.38(±0.37)
	TNR	86.48(±4.86)	89.07(±3.73)	90.73(±3.95)	44.71(±6.73)
	BACC	92.52(±2.37)	93.79(±1.92)	94.95(±1.98)	71.05(±3.40)
enn-s2s	TPR	98.63(±0.38)	98.63(±0.38)	98.74(±0.47)	98.74(±0.47)
	TNR	89.90(±4.98)	89.90(±4.98)	88.14(±3.67)	88.14(±3.67)
	BACC	94.27(±2.41)	94.27(±2.41)	93.44(±1.83)	93.44(±1.83)
Graph-CNN	TPR	98.94(±0.39)	98.94(±0.39)	98.91(±0.41)	98.91(±0.41)
	TNR	87.20(±3.33)	87.20(±3.33)	87.05(±4.18)	87.05(±4.18)
	BACC	93.07(±1.60)	93.07(±1.60)	92.98(±2.07)	92.98(±2.07)
GCN	TPR	98.98(±0.43)	98.47(±0.32)	99.08(±0.40)	97.37(±0.66)
	TNR	87.64(±3.47)	85.38(±5.10)	89.78(±3.77)	43.25(±6.68)
	BACC	93.31(±1.76)	91.93(±2.62)	94.43(±1.86)	70.31(±3.35)
CCGNet	TPR	99.82(±0.14)	99.78(±0.15)	99.78(±0.21)	99.24(±0.49)
	TNR	97.26(±1.61)	96.85(±1.45)	96.79(±1.35)	90.89(±3.55)
	BACC	98.54(±0.79)	98.31(±0.70)	98.28(±0.65)	95.07(±1.70)

<sup>a</sup> The model is trained on the inputs of c1-c2 and c2-c1.

<sup>b</sup> The model is trained only on the input of c1-c2.

**Supplementary Table 5.** Positive and negative co-crystal samples for nicotinamide in the independent test set.

Name	SMILES	Cocrystal	Ref
Fumaric Acid	<chem>O=C(O)/C=C/C(=O)O</chem>	Yes	EDAPOQ
Isonicotinamide	<chem>NC(=O)c1ccncc1</chem>	Yes	UMUYOR
Quercetin	<chem>O=c1c(O)c(-c2ccc(O)c(O)c2)oc2cc(O)cc(O)c12</chem>	Yes	NAFYUR
Adipic Acid	<chem>O=C(O)CCCC(=O)O</chem>	Yes	NUKYIC
Isoliquiritigenin	<chem>O=C(/C=C/c1ccc(O)cc1)c1ccc(O)cc1O</chem>	Yes	EYUGAI
3-Hydroxybenzoic Acid	<chem>O=C(O)c1cccc(O)c1</chem>	Yes	XAQQIQ
Anthranilic Acid	<chem>Nc1ccccc1C(=O)O</chem>	Yes	FEBSIR
Hydrochlorothiazide	<chem>NS(=O)(=O)c1cc2c(cc1Cl)NCNS2(=O)=O</chem>	Yes	PIRXUL
P-Coumaric Acid	<chem>O=C(O)/C=C/c1ccc(O)cc1</chem>	Yes	SOLBEC
Caffeic Acid Phenethyl Ester	<chem>O=C(/C=C/c1ccc(O)c(O)c1)OCCc1ccccc1</chem>	Yes	ETONIM
Tegafur	<chem>O=c1[nH]c(=O)n(C2CCCO2)cc1F</chem>	Yes	DOXDUR
Niflumic Acid	<chem>O=C(O)c1ccncc1Nc1cccc(C(F)(F)F)c1</chem>	Yes	EXAQEA
Ethylparaben	<chem>CCOC(=O)c1ccc(O)cc1</chem>	Yes	GOGQID
Febuxostat	<chem>Cc1nc(-c2ccc(OCC(C)C)c(C#N)c2)sc1C(=O)O</chem>	Yes	HIQQIJ
Mefenamic Acid	<chem>Cc1cccc(Nc2ccccc2C(=O)O)c1C</chem>	Yes	EXAQOK
DL-Ascorbic Acid	<chem>O=C1OC(C(O)CO)C(O)=C1O</chem>	Yes	OXOHEQ
Carbamazepine	<chem>NC(=O)N1c2ccccc2C=Cc2ccccc21</chem>	Yes	UNEZES
Tranilast	<chem>COc1ccc(/C=C/C(=O)Nc2ccccc2C(=O)O)cc1OC</chem>	Yes	KINTUY
(+/-)-Ivabradine	<chem>COc1cc2c(cc1OC)CC(=O)N(CCCN(C)CC1Cc3cc(OC)c(OC)cc31)CC2</chem>	No	1
MIs000678252	<chem>CC(=O)SC1CC2=CC(=O)CCC2(C)C2CCC3(C)C(CCC34CCC(=O)O4)C12</chem>	No	2
Nitazoxanide	<chem>CC(=O)Oc1ccccc1C(=O)Nc1ncc([N+](=O)[O-])s1</chem>	No	3
Ehrlich's reagent	<chem>CN(C)c1ccc(C=O)cc1</chem>	No	4
Famotidine	<chem>NC(N)=Nc1nc(CSCC/C(N)=N/S(N)(=O)=O)cs1</chem>	No	5
4-Methylbenzamide	<chem>Cc1ccc(C(N)=O)cc1</chem>	No	6
3-Methoxybenzamide	<chem>COc1cccc(C(N)=O)c1</chem>	No	6
2-Methoxybenzamide	<chem>COc1ccccc1C(N)=O</chem>	No	6
2-Methylbenzamide	<chem>Cc1ccccc1C(N)=O</chem>	No	6
Acetanilide	<chem>CC(=O)Nc1ccccc1</chem>	No	4
4-Methoxybenzoic Acid	<chem>COc1ccc(C(=O)O)cc1</chem>	No	6
3-Fluorobenzoic Acid	<chem>O=C(O)c1cccc(F)c1</chem>	No	6
3-Nitrobenzoic Acid	<chem>O=C(O)c1cccc([N+](=O)[O-])c1</chem>	No	6
Indole	<chem>c1ccc2[nH]ccc2c1</chem>	No	7

**Supplementary Table 6.** Positive and negative co-crystal samples for carbamazepine in the independent test set.

Name	SMILES	Cocrystal	Ref
4-Aminobenzoic Acid	<chem>Nc1ccc(C(=O)O)cc1</chem>	Yes	XAQRAJ
4-Hydroxybenzamide	<chem>NC(=O)c1ccc(O)cc1</chem>	Yes	SOGSEP
Hydroquinone	<chem>Oc1ccc(O)cc1</chem>	Yes	ABOQUF
Salicylic Acid	<chem>O=C(O)c1ccccc1O</chem>	Yes	MOXWAY
P-Benzoquinone	<chem>O=C1C=CC(=O)C=C1</chem>	Yes	UNEYOB
Nicotinamide	<chem>NC(=O)c1cccnc1</chem>	Yes	UNEZES
4-Nitropyridine N-Oxide	<chem>O=[N+][O-]c1cc[n+][O-]cc1</chem>	Yes	JIQKUS
Schembl5894079	<chem>ON1C=CN(O)c2ccccc21</chem>	Yes	VIGGOI
Fumaric Acid	<chem>O=C(O)/C=C/C(=O)O</chem>	Yes	WEYFEN
2,2,2-Trifluoroethanol	<chem>OCC(F)(F)F</chem>	Yes	SAPDUJ
Thiosaccharin	<chem>O=S1(=O)NC(=S)c2ccccc12</chem>	Yes	YAJGEY
Benzoic Acid	<chem>C1=CC=C(C=C1)C(=O)O</chem>	Yes	MOXVAX
Anthranilic Acid	<chem>C1=CC=C(C(=C1)C(=O)O)N</chem>	Yes	RUTGOE
Ketoprofen	<chem>CC(C(=O)O)c1cccc(C(=O)c2ccccc2)c1</chem>	Yes	RAFGEO
2-Hydroxyacetamide	<chem>NC(=O)CO</chem>	No	<sup>2</sup>
Lactamide	<chem>CC(O)C(N)=O</chem>	No	<sup>2</sup>
Glycolic Acid	<chem>O=C(O)CO</chem>	No	<sup>8</sup>
DL-Tartaric Acid	<chem>O=C(O)C(O)C(O)C(=O)O</chem>	No	<sup>8</sup>
Methylglucamine	<chem>CNCC(O)C(O)C(O)C(O)CO</chem>	No	<sup>2</sup>
Malic Acid	<chem>O=C(O)CC(O)C(=O)O</chem>	No	<sup>8</sup>
Malic Acid	<chem>O=C(O)CC(O)C(=O)O</chem>	No	<sup>8</sup>
Picolinamide	<chem>NC(=O)c1ccccn1</chem>	No	<sup>9</sup>

**Supplementary Table 7.** Positive and negative co-crystal samples for indomethacin in the independent test set.

<b>Cofomer</b>	<b>SMILES</b>	<b>Cocrystal</b>	<b>Ref</b>
Nicotinamide	<chem>NC(=O)c1ccnc1</chem>	Yes	SESKUY
Saccharin	<chem>O=C1NS(=O)(=O)c2ccccc21</chem>	Yes	UFERED
Neotam	<chem>COC(=O)C(Cc1cccc1)NC(=O)C(CC(=O)O)NCCC(C)(C)C</chem>	No	10
Vanillic Acid	<chem>COc1cc(C(=O)O)ccc1O</chem>	No	10
Cyclamic Acid	<chem>O=S(=O)(O)NC1CCCCC1</chem>	No	10
Glycine	<chem>NCC(=O)O</chem>	No	10
Oxalic Acid	<chem>O=C(O)C(=O)O</chem>	No	10
Fumaric Acid	<chem>C(=CC(=O)O)C(=O)O</chem>	No	10
Citric Acid	<chem>O=C(O)CC(O)(CC(=O)O)C(=O)O</chem>	No	10
Malic Acid	<chem>O=C(O)CC(O)C(=O)O</chem>	No	10
4-Aminobenzoic Acid	<chem>Nc1ccc(C(=O)O)cc1</chem>	No	10
Maleic Acid	<chem>O=C(O)/C=C\C(=O)O</chem>	No	10
Malonic Acid	<chem>O=C(O)CC(=O)O</chem>	No	10
Glutaric Acid	<chem>O=C(O)CCCC(=O)O</chem>	No	10
Urea	<chem>NC(N)=O</chem>	No	10
4-Aminobenzamide	<chem>NC(=O)c1ccc(N)cc1</chem>	No	10
4-Hydroxybenzoic Acid	<chem>O=C(O)c1ccc(O)cc1</chem>	No	10
Benzoic Acid	<chem>O=C(O)c1ccccc1</chem>	No	10
Succinic Acid	<chem>O=C(O)CCC(=O)O</chem>	No	10

**Supplementary Table 8.** Positive and negative co-crystal samples for paracetamol in the independent test set.

<b>Cofomer</b>	<b>SMILES</b>	<b>Cocrystal</b>	<b>Ref</b>
Phenazine	<chem>c1ccc2nc3ccccc3nc2c1</chem>	Yes	LUJSOZ
Theophylline	<chem>Cn1c(=O)c2[nH]cnc2n(C)c1=O</chem>	Yes	KIGLUI01
Oxalic Acid	<chem>O=C(O)C(=O)O</chem>	Yes	LUJTAM
Naphthalene	<chem>c1ccc2ccccc2c1</chem>	Yes	LUJSIT
Saccharin	<chem>O=C1NS(=O)(=O)c2ccccc21</chem>	No	11
DL-Ascorbic Acid	<chem>O=C1OC(C(O)CO)C(O)=C1O</chem>	No	12
Theobromine	<chem>Cn1cnc2c1c(=O)[nH]c(=O)n2C</chem>	No	11
Malonic Acid	<chem>O=C(O)CC(=O)O</chem>	No	11
Anthracene	<chem>c1ccc2cc3ccccc3cc2c1</chem>	No	13
Nicotinamide	<chem>NC(=O)c1ccnc1</chem>	No	14
Succinic Acid	<chem>O=C(O)CCC(=O)O</chem>	No	11
Adipic Acid	<chem>O=C(O)CCCCC(=O)O</chem>	No	11



**Supplementary Table 9.** Cocrystal samples (positive and negative ones) in the independent test set for Pyrene.

Cofomer	SMILES	Cocrystal	Ref
1,3,5-Trifluoro-2,4,6-Triiodobenzene	<chem>Fc1c(I)c(F)c(I)c(F)c1I</chem>	Yes	QEVWEW
Pyrazine-2,3,5,6-Tetracarbonitrile	<chem>N#Cc1nc(C#N)c(C#N)nc1C#N</chem>	Yes	BORPII
1,4-Dibromotetrafluorobenzene	<chem>Fc1c(F)c(Br)c(F)c(F)c1Br</chem>	Yes	GUQRAN
N-[2-(3-Methoxypropyl)Phenyl]Cyclohexanecarboxamide	<chem>N#Cc1c(O)c(C#N)c(C#N)c(O)c1C#N</chem>	Yes	TEXPOB
Naphthalene-1,4,5,8-Tetrone	<chem>O=c1ccc(=O)c2c(=O)ccc(=O)c1=2</chem>	Yes	CEKBUP
1,4-Diiodotetrafluorobenzene	<chem>Fc1c(F)c(I)c(F)c(F)c1I</chem>	Yes	FARNOD
Chlorothalonil	<chem>N#Cc1c(Cl)c(Cl)c(Cl)c(C#N)c1Cl</chem>	Yes	HAYYOW
Iodopentafluorobenzene	<chem>Fc1c(F)c(F)c(I)c(F)c1F</chem>	Yes	GUQQIU
Tetrachloroterephthalonitrile	<chem>N#Cc1c(Cl)c(Cl)c(C#N)c(Cl)c1Cl</chem>	Yes	WAWPAM
1,3-Dibromotetrafluorobenzene	<chem>Fc1c(F)c(Br)c(F)c(Br)c1F</chem>	Yes	GUQQUG
F4-Tcnq	<chem>N#CC(C#N)=c1c(F)c(F)c(=C(C#N)C#N)c(F)c1F</chem>	Yes	MIDDEL
1,2-Dibromotetrafluorobenzene	<chem>Fc1c(F)c(F)c(Br)c(Br)c1F</chem>	Yes	GUQQA
Hexafluorobenzene	<chem>Fc1c(F)c(F)c(F)c(F)c1F</chem>	Yes	ZZZGKE01
1,3,5-Tribromo-2,4,6-Trifluorobenzene	<chem>Fc1c(Br)c(F)c(Br)c(F)c1Br</chem>	Yes	QEVXOH
P-Benzoquinone	<chem>O=C1C=CC(=O)C=C1</chem>	Yes	PYRBZQ
4,5-Dibromophthalic Anhydride	<chem>O=C1OC(=O)c2cc(Br)c(Br)cc21</chem>	Yes	EHESUF
Picric Acid	<chem>O=[N+](=[O-])c1cc([N+](=O)[O-])c(O)c([N+](=O)[O-])c1</chem>	Yes	PYRPCT02
Bromopentafluorobenzene	<chem>Fc1c(F)c(F)c(Br)c(F)c1F</chem>	Yes	GUQQEQ
2309-49-1	<chem>Cn1c(=O)c2c(n(C)c1=O)n(C)c(=O)n2C</chem>	Yes	MURPYR
Tetrafluoro-1,4-Benzoquinone	<chem>O=C1C(F)=C(F)C(=O)C(F)=C1F</chem>	Yes	PYRFLR
Tetracyanoethylene	<chem>N#CC(C#N)=C(C#N)C#N</chem>	Yes	PYRCYE10
4,7-Dibromobenzo(C)Furazan 1-Oxide	<chem>Brc1c2=NON(=c2c(Br)cc1)O</chem>	Yes	AYEGAM
917-23-7	<chem>C1=Cc2nc1c(-c1ccccc1)c1ccc([nH]1)c(-c1ccccc1)c1nc(c(-c3ccccc3)c3ccc([nH]3)c2-c2ccccc2)C=C1</chem>	Yes	XAGMAT
Hexachlorobenzene	<chem>Clc1c(Cl)c(Cl)c(Cl)c(Cl)c1Cl</chem>	Yes	ISISAG
Benzene-1,2,4,5-Tetracarbonitrile	<chem>N#Cc1cc(C#N)c(C#N)cc1C#N</chem>	Yes	PYRCBZ
Chloranil	<chem>O=C1C(Cl)=C(Cl)C(=O)C(Cl)=C1Cl</chem>	Yes	PYRCLN
Tetrachlorophthalonitrile	<chem>N#Cc1c(Cl)c(Cl)c(Cl)c(Cl)c1C#N</chem>	Yes	PINJUU02

Octafluoronaphthalene	<chem>Fc1c(F)c(F)c2c(F)c(F)c(F)c(F)c2c1F</chem>	Yes	ECUVIH
9-(4-Methoxyphenyl)Xanthene-9-Ol	<chem>COc1ccc(C2(O)c3ccccc3Oc3ccccc32)cc1</chem>	Yes	XETTEW
1487-82-7	<chem>Cc1cc(=C(C#N)C#N)c(C)cc1=C(C#N)C#N</chem>	Yes	VOQCUC
34151-49-0	<chem>O=C1c2ccc3c4c(ccc(e24)C(=O)N1c1ccnc1)C(=O)N(c1ccnc1)C3=O</chem>	Yes	GUMNUY
N,-N'-Dimethylpyromellitic Acid Diimide	<chem>Cn1c(=O)c2cc3c(=O)n(C)c(=O)c3cc2c1=O</chem>	Yes	PAYYOG
N,N'-(1,3,6,8-Tetraoxo-1,3,6,8-Tetrahydrobenzo[Lmn][3,8]Phenanthroline-2,7-Diyl)Diisonicotinamide	<chem>O=C(NN1C(=O)c2ccc3c4c(ccc(e24)C1=O)C(=O)N(NC(=O)c1ccnc1)C3=O)c1ccnc1</chem>	Yes	OPUQUN
Nsc97081	<chem>CCN1C(=O)/C(=C2\SC(=S)N(CC)C2=O)SC1=S</chem>	Yes	QOLQOA
2-Chloro-1,4-Benzoquinone	<chem>O=C1C=CC(=O)C(Cl)=C1</chem>	Yes	CORPIJ
3-Propyl-5-[3-Propyl-2,4-Bis(Sulfanylidene)-1,3-Thiazolidin-5-Ylidene]-1,3-Thiazolidine-2,4-Dithione	<chem>CCCN1C(=S)S/C(=C2/SC(=S)N(CCC)C2=S)C1=S</chem>	Yes	QOLQEQ
2-Chloro-11,11,12,12-Tetracyanoanthraquinodimethane	<chem>N#CC(C#N)=c1c2ccccc2c(=C(C#N)C#N)c2cc(Cl)ccc12</chem>	Yes	GAFJAY
Bromanil	<chem>O=C1C(Br)=C(Br)C(=O)C(Br)=C1Br</chem>	Yes	REDFIP
1518-16-7	<chem>N#CC(C#N)=c1ccc(=C(C#N)C#N)cc1</chem>	Yes	BITBUD
O-Chloranil	<chem>O=C1C(=O)C(Cl)=C(Cl)C(Cl)=C1Cl</chem>	Yes	REQVOZ
2-(3,4-Diethoxy-2,5-Dioxo-3-Cyclopenten-1-Ylidene)-Malononitrile	<chem>CCOC1=C(OCC)C(=O)C(=C(C#N)C#N)C1=O</chem>	Yes	BEFGIC
5,6-Dibromobenzofurazane 1-Oxide	<chem>[O-][n+]1onc2cc(Br)c(Br)cc21</chem>	Yes	EHESIT
Zinc361240	<chem>Cc1ccc(S(=O)(=O)N=C2C=C(Cl)C(=O)C(Cl)=C2)cc1</chem>	Yes	PYTQIM
2-Bromo-1,3,5-Trinitrobenzene	<chem>O=[N+]([O-])c1cc([N+](=O)[O-])c(Br)c([N+](=O)[O-])c1</chem>	Yes	PYRBPC
Chloropentafluorobenzene	<chem>Fc1c(F)c(F)c(Cl)c(F)c1F</chem>	Yes	GUQQAM
98507-06-3	<chem>CC1=C/C(=N\C#N)C(C)=C/C1=N\C#N</chem>	Yes	VOQDAJ
9,9'-Bifluorenylidene	<chem>c1ccc2c(c1)C(=C1c3ccccc3-c3ccccc31)c1ccccc1-2</chem>	Yes	CUNWUD
Pyromellitic Dianhydride	<chem>O=c1oc(=O)c2cc3c(=O)oc(=O)c3cc12</chem>	Yes	PYRPMA01
3-Ethyl-5-(3-Ethyl-2-Oxo-4-Sulfanylidene-1,3-Thiazolidin-5-Ylidene)-4-Sulfanylidene-1,3-Thiazolidin-2-One	<chem>CCN1C(=O)S/C(=C2/SC(=O)N(CC)C2=S)C1=S</chem>	Yes	QOLRER

3-Ethyl-5-[3-Ethyl-2,4-Bis(Sulfanylidene)-1,3-Thiazolidin-5-Ylidene]-1,3-Thiazolidine-2,4-Dithione	<chem>CCN1C(=S)S/C(=C2/SC(=S)N(CC)C2=S)C1=S</chem>	Yes	QOLPUF
3,3',5,5'-Tetrabromo-1,1'-Bi(Cyclohexa-2,5-Dien-1-Ylidene)-4,4'-Dione	<chem>O=C1C(Br)=CC(=C2C=C(Br)C(=O)C(Br)=C2)C=C1Br</chem>	Yes	BAZCUA
13-Methyl-6,7,8,9,11,12,14,15,16,17-Decahydrocyclopenta[A]Phenanthrene-3,17-Diol	<chem>CC12CCC3c4ccc(O)cc4CCC3C1CCC2O</chem>	Yes	CUTBEZ
3,3',5,5'-Tetrachlorodiphenoquinone	<chem>O=C1C(Cl)=CC(=C2C=C(Cl)C(=O)C(Cl)=C2)C=C1Cl</chem>	Yes	BAZDAH
1,8-Dinitroanthraquinone	<chem>O=C1c2cccc([N+](=O)[O-])c2C(=O)c2c1cccc2[N+](=O)[O-]</chem>	Yes	AGORAS
Methyl Picrate	<chem>COc1c([N+](=O)[O-])cc([N+](=O)[O-])cc1[N+](=O)[O-]</chem>	Yes	CILRAQ
17-Acetyl-10,13-Dimethyl-1,2,6,7,8,9,11,12,14,15,16,17-Dodecahydrocyclopenta[A]Phenanthren-3-One	<chem>CC(=O)C1CCC2C3CCC4=CC(=O)CCC4(C)C3CCC12C</chem>	Yes	CUSZUM
9,10-Dicyanoanthracene	<chem>N#Cc1c2cccc2c(C#N)c2cccc12</chem>	Yes	EHUFEV
6H-Benzo[C]Chromen-6-One	<chem>O=c1oc2cccc2c2cccc12</chem>	Yes	EHUFIZ
Carbazole	<chem>c1ccc2c(c1)[nH]c1cccc12</chem>	No	15
Anthracene	<chem>c1ccc2cc3cccc3cc2c1</chem>	No	16
Chrysene	<chem>c1ccc2c(c1)ccc1c3cccc3ccc21</chem>	No	15
Phenanthrene	<chem>c1ccc2c(c1)ccc1cccc12</chem>	No	15
Naphthalene	<chem>c1ccc2cccc2c1</chem>	No	15
Fluoranthene	<chem>c1ccc2c(c1)-c1cccc3cccc-2c13</chem>	No	15

**Supplementary Table 10.** Performances of all the models on the independent test sets of TNT and CL-20 without the transfer learning.

	Metrics	SVM	RF	DNN-desc	DNN-FP	enn-s2s	Graph-CNN	GCN	CCGNet
TNT	TPR (%)	78.26	69.57	95.65	0	65.22	65.22	60.87	95.65
	TNR (%)	12.50	12.50	25	65.22	37.5	37.5	37.5	25
	BACC (%)	45.38	41.03	60.33	32.61	51.36	51.36	49.18	60.33
CL-20	TPR (%)	77.78	83.33	100	0	100	100	100	100
	TNR (%)	16.67	33.33	16.67	100	0	0	0	0
	BACC (%)	47.22	58.33	58.33	50	50	50	50	50

**Supplementary Table 11.** Refcodes for 116 positive samples of energetic cocrystals used in this work, collected from Cambridge Structural Database.

REDCIM	LUTGUD	POCVIP	XIZCER	ABUNIU	PYRTNB
JABYIX	SUGCAY	WIFYAN	PUTXAF	REDDAF	HETTOS
RULLUF	ZEVNUL	RENPUV	PUTXEJ	ZUBNUH	ZEGKIF10
ANCTNB	ZASWAT	SERZIB	WOSFOB	QOSRUN	YOJXON
CAZTBZ01	DUKBOC	APANBZ	KUMYOI	PUTWOS	ABTNBA01
KOBFIQ	VIGLEC	WOJXEY	VAZBIJ	BOXTET	YOJQOG
JOCTAZ	ZEZHAP	NIKLOL	GEXMIH	JAQVOP	POSREV
VIGKIF	WOJWIB	FUFSOQ	SKTNIB	ROSMOD	QARQUY
UGUNAN	ZILMUF	UTEJAG	WIFXUG	GEXMON	NILCET
GOWHIL	BNZTNB	WUGWAY	RUYLAY	FONJAV	AJAKOL
PUTWEI	ZEZGIW	PUBWEO	CECFEF	HUZSEA	PVVBF01
NIBZAM	XEMCID	WEPTAP	HETTUY	SOQPAQ	MEPWIQ
ZEZGOC	USEZID	STINBZ	RUYKUR	PUTWIM	FOYSUJ
PUTWUY	YOJXIH	QOWBEJ	DUKBUI	MAAZNB	ZEZHOD
KIZVAQ	MANLEV	ROSMIX	GEXMED	ERAFAE	XAHZAH
CEZFOF	HETTIM	ZOPGOC	JOCSEC	JAQXUX	URILIR
HECREM	LOKJIH	JAQXOR	ZUBNOB	TIVJUF	QAPNAZ
URILUD	VIGKUR	REDDEJ	BZATNB20	PUBMUU20	DUKCAP
ZZZAGS10	ZEZHET	REDCUY	RUYLEC	PVVBKP01	CBZTNB
WOJWOH	IDENEM				

**Supplementary Table 12.** The ISPE (kJ/mol) values of 864 coformer pairs computed in this work.

	<b>RDX</b>	<b>HNS</b>	<b>TATB</b>	<b>DAAF</b>	<b>DAOAF</b>	<b>DATB</b>	<b>LLM-105</b>	<b>FOX-7</b>	<b>NQ</b>
<b>1-4-DNI</b>	-2.81	-0.39	-0.56	-1.27	-1.41	-1.33	-0.14	-13.12	-5.37
<b>1-BN</b>	-3.11	-5.46	-3.67	-1.18	-1.48	-5.01	-2.83	-3.63	-1.80
<b>2-4-DNI</b>	-1.34	-0.25	-0.19	-2.58	-2.86	-1.25	-1.68	-15.79	-6.69
<b>2-4-MDNI</b>	-3.48	-1.14	-0.07	-1.18	-1.09	-1.09	-0.48	-11.86	-4.38
<b>3-4-DNP</b>	-1.25	-1.31	-0.09	-2.52	-2.39	-0.14	-2.75	-12.64	-6.07
<b>3-4-MDNP</b>	-6.21	-5.47	-0.83	-1.79	-1.24	-2.80	-2.33	-7.14	-2.61
<b>3-5-DNP</b>	-1.61	-0.70	-0.22	-3.15	-3.11	-0.48	-3.33	-15.22	-6.88
<b>3-AT</b>	-1.88	-2.85	-1.86	-1.58	-1.59	-2.20	-2.92	-5.50	-3.82
<b>4-5-MDNI</b>	-5.82	-5.08	-1.02	-1.29	-0.96	-2.22	-2.20	-6.24	-2.21
<b>4-5-MDNP</b>	-2.89	-2.21	-0.09	-0.74	-0.34	-0.50	-0.74	-9.46	-3.50
<b>4-AT</b>	-0.26	-0.05	-0.47	0.01	-0.36	-0.48	-0.07	-5.29	-3.86
<b>9-BN</b>	-4.89	-8.49	-7.50	-1.50	-3.36	-9.09	-4.34	-3.64	-1.90
<b>A12</b>	-6.19	-7.39	-3.17	-4.12	-3.63	-5.55	-4.58	-4.23	-2.94
<b>A3</b>	-7.39	-6.78	-2.10	-4.85	-4.04	-4.62	-4.58	-5.94	-2.52
<b>A4</b>	-8.89	-8.10	-2.84	-5.99	-5.29	-5.82	-5.93	-5.69	-3.24
<b>A5</b>	-7.70	-6.19	-3.11	-3.85	-4.17	-5.20	-4.53	-3.23	-1.74
<b>A7</b>	-7.83	-6.87	-2.17	-5.24	-4.50	-4.78	-4.98	-6.02	-2.95
<b>A8</b>	-9.85	-5.94	-1.56	-4.39	-3.47	-4.13	-4.44	-0.13	-0.08
<b>AA_1</b>	-3.06	-4.78	-3.09	-0.72	-1.40	-4.03	-2.54	-7.97	-4.70
<b>ADNP</b>	-2.13	-2.61	-0.10	-2.26	-1.97	-0.73	-2.43	-12.38	-5.16
<b>alpha-ABA_1</b>	-9.09	-10.40	-9.44	-5.13	-6.63	-10.30	-8.26	-12.34	-8.16
<b>ANAT</b>	-6.35	-5.80	-3.46	-4.73	-4.30	-4.77	-5.61	-1.65	-1.14
<b>Ant</b>	-4.27	-8.93	-6.64	-2.19	-2.47	-8.64	-3.97	-2.55	-1.65
<b>AT</b>	-0.22	-0.41	-0.06	-0.02	-0.09	-0.06	-0.11	-3.98	-2.17
<b>ATNO2</b>	-2.83	-1.91	-1.22	-2.59	-2.99	-2.00	-3.17	-6.26	-5.32
<b>ATZ</b>	-0.26	-0.05	-0.47	0.01	-0.36	-0.48	-0.07	-5.29	-3.86
<b>AZ1</b>	-1.20	-2.61	-3.61	-3.02	-3.58	-2.66	-3.72	-17.44	-6.97
<b>AZ2</b>	-1.11	-2.87	-2.65	-1.40	-1.77	-2.50	-2.51	-14.40	-6.01
<b>Benzene-1-2-diamine</b>	-2.11	-2.05	-0.06	-0.09	0.00	-0.07	-0.44	-5.61	-1.86
<b>BL</b>	-5.61	-4.37	-1.70	-4.97	-4.41	-3.44	-4.28	-7.35	-5.28
<b>BQ</b>	-5.10	-5.28	-0.55	-1.93	-1.10	-2.31	-1.77	-6.49	-2.26
<b>BTF</b>	-6.10	-5.56	-6.60	-4.07	-5.50	-6.81	-5.30	-18.41	-8.05
<b>BTO</b>	-3.19	-1.85	-3.97	-3.09	-3.43	-4.31	-1.59	-23.41	-6.78
<b>CE</b>	-1.18	-0.59	-1.67	-0.20	-0.80	-1.21	-0.13	-15.37	-4.88
<b>CIM</b>	-2.47	-0.21	-0.06	-1.32	-1.36	-0.13	-0.86	-6.56	-4.36
<b>CL-20</b>	-7.21	-7.45	-15.12	-11.52	-13.00	-12.19	-11.64	-34.22	-13.81
<b>CPL</b>	-4.26	-1.70	-0.08	-4.01	-3.87	-1.64	-3.78	-7.41	-4.88

<b>DADP</b>	-9.36	-10.79	-4.91	-3.14	-1.94	-6.72	-5.12	-2.41	-0.36
<b>DAF</b>	-3.40	-1.84	-1.96	-1.37	-1.87	-2.32	-1.53	-6.36	-5.32
<b>DANA</b>	-4.04	-3.53	-0.09	-0.98	-0.37	-0.87	-1.06	-7.83	-2.90
<b>DAT</b>	-6.03	-4.91	-1.70	-2.23	-1.74	-2.63	-2.83	-3.91	-1.91
<b>D-explosive</b>	-1.57	-0.19	-1.02	-1.09	-1.07	-1.43	-0.22	-17.03	-5.14
<b>DMB</b>	-6.46	-10.70	-4.26	-1.91	-0.95	-6.72	-3.52	-3.36	-0.68
<b>DMF</b>	-6.80	-5.19	-2.42	-6.10	-5.71	-4.33	-5.60	-7.94	-5.93
<b>DMI</b>	-8.90	-7.83	-4.09	-7.62	-7.18	-6.50	-7.95	-9.00	-6.86
<b>DNB</b>	-2.92	-1.99	-0.08	-0.75	-0.16	-0.40	-0.66	-9.64	-3.24
<b>DNBT</b>	-0.71	-0.22	-0.06	-1.68	-1.72	-0.40	-1.32	-15.72	-5.03
<b>DNDA</b>	-5.93	-5.09	-0.66	-1.69	-1.08	-2.31	-1.93	-6.62	-2.29
<b>DNP</b>	-5.93	-5.09	-0.66	-1.69	-1.08	-2.31	-1.93	-6.61	-2.29
<b>DNPP</b>	-2.78	-3.70	-1.14	-3.52	-3.64	-0.58	-4.58	-16.52	-7.21
<b>DNT</b>	-3.44	-2.69	-0.11	-0.91	-0.42	-0.38	-0.82	-9.49	-3.32
<b>DNTF</b>	-2.46	-1.41	-3.35	-1.42	-2.25	-2.79	-0.98	-17.89	-5.97
<b>DO</b>	-7.44	-7.43	-3.61	-4.42	-3.49	-5.38	-5.31	-2.76	-0.43
<b>EDNA</b>	-2.43	-3.04	-0.09	-2.50	-2.01	-0.95	-2.96	-11.43	-5.16
<b>FA</b>	-7.68	-4.15	-1.07	-5.45	-4.99	-3.68	-4.25	-6.14	-5.50
<b>GTA</b>	-10.94	-11.11	-4.09	-5.33	-4.16	-7.45	-5.31	-4.21	-1.24
<b>HMX</b>	-0.38	-0.65	-0.15	-0.05	-0.12	-0.62	-0.15	-10.95	-3.22
<b>MAM</b>	-5.67	-6.53	-1.78	-2.27	-1.44	-3.53	-3.06	-3.24	-0.88
<b>MATNB</b>	-1.47	-1.90	-0.20	-0.64	-0.35	-0.55	-0.68	-11.37	-4.46
<b>MDNT</b>	-2.51	-0.37	-0.23	-0.62	-0.63	-0.74	-0.21	-13.60	-4.61
<b>MNO</b>	-2.72	-1.62	-0.12	-1.45	-1.15	-1.06	-0.87	-11.93	-4.28
<b>MTNP</b>	-1.50	-0.44	-0.81	-0.11	-0.43	-0.62	-0.45	-12.28	-4.28
<b>Nap</b>	-4.57	-9.63	-6.72	-2.37	-2.64	-8.68	-4.29	-2.01	-1.55
<b>NAQ</b>	-4.78	-4.96	-1.01	-2.48	-1.80	-2.85	-2.68	-5.39	-1.74
<b>NMP</b>	-8.72	-6.77	-4.01	-7.85	-7.34	-6.00	-7.87	-8.27	-6.67
<b>NN</b>	-5.84	-5.59	-1.48	-3.16	-2.56	-3.31	-3.21	-4.91	-1.74
<b>NTO</b>	-1.46	-0.56	-0.76	-2.53	-2.72	-0.96	-2.43	-15.44	-6.76
<b>PA</b>	-1.57	-0.19	-1.02	-1.09	-1.07	-1.43	-0.22	-17.03	-5.14
<b>PDA</b>	-2.30	-2.24	-0.25	-0.28	-0.19	-0.26	-0.63	-5.80	-2.06
<b>PDCA</b>	-6.22	-8.32	-5.97	-2.85	-3.44	-6.80	-5.20	-6.45	-3.97
<b>Per</b>	-4.99	-9.26	-6.81	-2.41	-3.06	-8.75	-4.60	-3.91	-2.36
<b>PETN</b>	-3.50	-3.12	-3.34	-1.63	-2.83	-3.95	-2.16	-14.87	-5.09
<b>phenanthrene</b>	-3.28	-8.17	-5.00	-1.34	-1.46	-6.99	-2.91	-2.96	-2.28
<b>Pnox</b>	-10.93	-8.90	-3.43	-8.55	-7.85	-6.81	-7.69	-6.70	-5.37
<b>Py</b>	-3.86	-2.66	-0.81	-2.02	-1.59	-1.75	-1.88	-1.93	-0.28
<b>Pyr</b>	-1.80	-5.54	-2.96	-0.14	-0.15	-4.52	-1.19	-3.24	-0.58
<b>TBTNB</b>	-1.32	-0.76	-1.01	-0.37	-0.81	-1.16	-0.95	-12.01	-3.44
<b>TCTNB</b>	-0.89	0.06	0.28	-0.16	-0.44	-0.45	-0.66	-10.73	-3.17
<b>TITNB</b>	-2.53	-4.19	-4.03	-1.13	-1.89	-4.14	-2.68	-12.98	-4.45
<b>TNA</b>	-0.96	-0.47	-0.42	-0.58	-0.55	-0.69	-0.52	-14.80	-4.84
<b>TNAN</b>	-1.01	-0.63	-0.18	-0.67	-0.55	-0.69	0.03	-13.04	-4.02

<b>TNAZ</b>	-1.44	-0.52	-2.94	-1.01	-1.97	-2.65	-1.22	-18.76	-6.11
<b>TNB</b>	-1.61	-1.00	-0.93	-0.91	-1.31	-1.74	-0.79	-12.98	-4.17
<b>TNGU</b>	-5.17	-5.83	-7.71	-6.10	-8.40	-7.69	-8.78	-22.30	-9.57
<b>TNT</b>	-0.91	-0.24	-0.50	-0.60	-0.55	-0.77	0.01	-14.42	-4.35
<b>TTNB</b>	-3.43	-4.83	-6.16	-0.70	-1.83	-7.54	-2.36	-9.02	-3.28
<b>TZTN</b>	-4.07	-1.94	-0.69	-3.01	-3.17	-2.04	-3.06	-11.61	-6.02
<b>xylene</b>	-3.68	-5.88	-3.47	-0.96	-0.79	-4.48	-2.93	-1.64	-0.02
<b>RDX</b>	--	-1.33	-3.07	-0.78	-0.85	-2.09	-0.91	-19.28	-5.41
<b>HNS</b>	-1.33	--	-1.05	-1.23	-1.21	-1.60	0.18	-17.16	-4.86
<b>TATB</b>	-3.07	-1.05	--	-0.55	-0.10	-0.27	-0.27	-9.17	-2.86
<b>DAAF</b>	-0.78	-1.23	-0.55	--	-0.03	-0.42	-0.37	-10.41	-4.22
<b>DAOAF</b>	-0.85	-1.21	-0.10	-0.03	--	-0.08	-0.08	-9.36	-3.72
<b>DATB</b>	-2.09	-1.60	-0.27	-0.42	-0.08	--	0.08	-13.25	-3.90
<b>LLM-105</b>	-0.91	0.18	-0.27	-0.37	-0.08	0.08	--	-11.50	-4.12
<b>FOX-7</b>	-19.28	-17.16	-9.17	-10.41	-9.36	-13.25	-11.50	--	-1.65
<b>NQ</b>	-5.41	-4.86	-2.86	-4.22	-3.72	-3.90	-4.12	-1.65	--

---

**Supplementary Table 13.** Performance of the best 10 CCGNet models.

<b>Model</b>	<b>Loss</b>	<b>Valid Accuracy</b>
1	0.00037	1.0
2	0.00042	1.0
3	0.00055	1.0
4	0.00122	1.0
5	0.00272	1.0
6	0.00368	1.0
7	0.00412	1.0
8	0.00673	1.0
9	0.00977	1.0
10	0.02454	1.0



**Supplementary Table 14.** Heats of formation for H, C, O and N atoms.

---

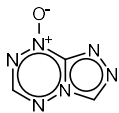
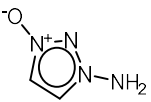
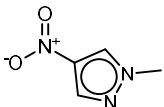
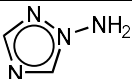
Atoms	$H_{(\text{atoms},298)}^{\circ}$ [a.u.] <sup>a</sup> (Hartree/Particle)	$\Delta H_{f(\text{atoms},298)}^{\circ}$ <sup>b</sup> (kJ/mol)
H	-0.500991	218.2
C	-37.786156	717.2
O	-74.991202	249.5
N	-54.522462	473.1

---

<sup>a</sup> the calculated values by CBS-4M method

<sup>b</sup> the experimental values<sup>17</sup>

**Supplementary Table 15.** The impact sensitivity and heat of explosion calculated for cofomers 5, 7, 8, 10.

<b>Cofomers</b>	<b>Impact Sensitivity (IS)</b>	<b>Heat of explosion (Q, cal/g)</b>
 Cofomer 5	1.5941	$1.483 \times 10^3$
 Cofomer 7	2.3146	$1.484 \times 10^3$
 Cofomer 8	2.8939	$1.174 \times 10^3$
 Cofomer 10	6.2555	$0.797 \times 10^3$

**Supplementary Table 16.** Crystal data and structure refinement for CL-20/1-Methyl-4-nitropyrazole cocrystal.

<b>CCDC no.</b>	2107286
<b>Empirical formula</b>	C <sub>10</sub> H <sub>11</sub> N <sub>15</sub> O <sub>14</sub>
<b>Formula weight</b>	565.34
<b>Temperature</b>	296 K
<b>Crystal system</b>	Orthorhombic
<b>Space group</b>	Pbca
<b>Unit cell dimensions</b>	a = 11.9344(12) Å    a = 90° b = 10.9427(10) Å    b = 90° c = 31.436(3) Å    γ = 90°
<b>Volume</b>	4105.4(7) Å <sup>3</sup>
<b>Z</b>	8
<b>Density (calculated)</b>	1.829 g/cm <sup>3</sup>
<b>Absorption coefficient</b>	0.170 mm <sup>-1</sup>
<b>F(000)</b>	2304
<b>Crystal size</b>	0.33 x 0.3 x 0.28 mm <sup>3</sup>
<b>Theta range for data collection</b>	2.143 to 30.466°.
<b>Index ranges</b>	-16 ≤ h ≤ 17, -15 ≤ k ≤ 11, -44 ≤ l ≤ 44
<b>Reflections collected</b>	39289
<b>Independent reflections</b>	6237 [R(int) = 0.0290]
<b>Completeness to theta = 25.242°</b>	99.90%
<b>Absorption correction</b>	Semi-empirical from equivalents
<b>Max. and min. transmission</b>	0.7461 and 0.6897
<b>Refinement method</b>	Full-matrix least-squares on F <sup>2</sup>
<b>Data / restraints / parameters</b>	6237/0/353
<b>Goodness-of-fit on F<sup>2</sup></b>	1.043
<b>Final R indices [I &gt; 2σ(I)]</b>	R <sub>1</sub> = 0.0480, wR <sub>2</sub> = 0.1171
<b>R indices (all data)</b>	R <sub>1</sub> = 0.0640, wR <sub>2</sub> = 0.1282
<b>Extinction coefficient</b>	n/a
<b>Largest diff. peak and hole</b>	0.312 and -0.351 e.Å <sup>-3</sup>

# Supplementary Discussion

## Attention Visualization

The interpretability of the deep learning model has been a challenge. Herein, we introduce the attention mechanism to further optimize the feature space on one side, and make the model interpretable on the other side. The attention can weight important patterns associated with the target property. Supplementary Figure 1 representatively selects some cocrystals to exemplify, where the attention weights are mapped to corresponding atoms in 2D structures, in turn visualizing some important patterns hidden under the data. For WAWDEE (Cambridge Structural Database refcode) in Supplementary Figure 1(a), the attention weights highlight on the nitrogen atoms and hydroxy groups involving the intermolecular H-bonding and the benzene ring involving the weak intermolecular  $\pi$ - $\pi$  interaction with the pyrimidine ring. The crystal structure of KARHAM shows that the co-crystallization is mainly driven by the intermolecular  $\pi$ - $\pi$  stack while the attention coefficients just capture these groups involving the interaction, as reflected by the 2D structure in Supplementary Figure 1(b). The other examples in Supplementary Figure 1 similarly reflect that the attention weights can capture the atoms and groups involving the important interactions between a pair of cofomers.

# Supplementary Methods

## Construction and Bayesian optimization of the competitive models

In the section, we briefly describe the construction of the seven competitive models and Bayesian optimization on their hyper-parameters, along with their best configurations determined by the optimization.

**RF and SVM** are conventional machine learning (ML) models. RF (Random Forest) is an ensemble learning method that contains multiple decision trees. For the classification task, the output of RF is the class selected by most trees. SVM (support-vector machine) is a supervised learning model for the classification and regression. SVM maps training samples to points in space so as to maximize the width of the gap between the two classes. New samples are then mapped into that same space and predicted to belong to a class based on which side of the gap they fall. We implement RF and SVM by using Scikit-learn<sup>18</sup>.

**DNN-FP and DNN-desc** are Deep Neural Networks composed of dense layers. DNN-FP is also derived from the work of Devogelaer et al<sup>19</sup> and used the extended-connectivity fingerprints (ECFP) as the feature descriptor. Following Ref.<sup>19</sup>, we build its framework (see Ref.<sup>19</sup> for more details). For DNN-desc, it is constructed by sequential dense layers and adopts the concatenation of the 12 molecular descriptors of a pair of conformer as input. DNN-FP and DNN-desc are implemented by TensorFlow<sup>20</sup>.

**Graph-CNN** is a spatial-based graph convolution network proposed by Felipe et al<sup>21</sup>, where key components are Graph-CNN layers and Graph Embedding Pooling (GEP) layers. The two kinds of layers perform the message passing phase. The readout phase is a flattening operation. Excepting for the final output layer, batch normalization<sup>22</sup> and ReLU<sup>23</sup> are applied in each layer. Since the graph convolution of our CCGblock follows the Graph-CNN layer framework (see Methods in the text for details of Graph-CNN layer). Here we mainly introduce the GEP layer, as shown in Supplementary Figure 4.

Like pooling layers in conventional CNNs, the GEP layer is used to reduce dimensions of the input, which eliminates redundant information and also improves performance of computation. GEP transfers a graph with node number  $N$  to a given number  $N'$ . For this purpose, an embedding matrix  $\mathbf{X}_{\text{emb}} \in \mathbb{R}^{N \times N'}$  is produced by a filter tensor  $\mathbf{H}_{\text{emb}} \in \mathbb{R}^{N \times N \times C \times N'}$ . The calculation of  $\mathbf{X}_{\text{emb}}$  is similar to the multiple filters Graph-CNN (vide Methods), where the learnable filter  $\mathbf{H}_{\text{emb}}$  is multiplied by the node features  $\mathbf{X}_{\text{in}}$ . It is defined by Supplementary Equations (1-2):

$$\mathbf{x}_{\text{emb}}^{(n')} = \sum_{c=1}^C \mathbf{H}_{\text{emb}}^{(c,n')} \mathbf{x}_{\text{in}}^{(c)} + b \quad (1)$$

$$\mathbf{X}_{\text{emb}} = \text{softmax}(\text{GConv}_{\text{emb}}(\mathbf{X}_{\text{in}}, N') + \mathbf{b}) \quad (2)$$

where  $\mathbf{H}_{\text{emb}}^{(c,n')} \in \mathbb{R}^{N \times N}$  is a part of  $\mathbf{H}_{\text{emb}}$ .  $\mathbf{x}_{\text{emb}}^{(n')}$  is a column of  $\mathbf{X}_{\text{emb}} \in \mathbb{R}^{N \times N'}$ . The pooled graph data will be calculated by the next operations (Supplementary Equations (3-4)).

$$\mathbf{X}_{\text{out}} = \mathbf{X}_{\text{emb}}^T \mathbf{X}_{\text{in}} \quad (3)$$

$$\mathbf{A}_{\text{out}} = \mathbf{X}_{\text{emb}}^T \mathbf{A}_{\text{in}} \mathbf{X}_{\text{emb}} \quad (4)$$

where  $\mathbf{A}_{\text{in}} \in \mathbb{R}^{N \times N}$  is adjacency matrix,  $\mathbf{A}_{\text{out}} \in \mathbb{R}^{N' \times N'}$  is pooled adjacency matrix.  $\mathbf{X}_{\text{out}} \in \mathbb{R}^{N' \times C}$  is pooled node feature matrix. Finally, a pooled graph that has  $\mathbf{A}_{\text{out}}$  and  $\mathbf{X}_{\text{out}}$  is produced by GEP. Graph-CNN is built by using TensorFlow<sup>20</sup>.

**enn-s2s**, proposed by Gilmer et al<sup>24</sup>, has two phases (a message passing phase and a readout phase), as shown in Supplementary Figure 6(g). In Gilmer's work, enn-s2s is a regression model. Here, in order to extend its application to the classification prediction of the cocrystal formation, we modified the architecture of enn-s2s by changing the dimension of output layer. The message passing phase includes two functions, *i.e.*, message passing function and update function. The message passing function is used to propagate node features, as reflected by Supplementary Equation (6).

$$\mathbf{x}_i^t = \mathbf{W} \mathbf{x}_i^{t-1} + \sum_{j \in \mathcal{N}(i)} \mathbf{x}_j^{t-1} \cdot \text{MLP}(\mathbf{e}_{i,j}) \quad (5)$$

Where  $\mathbf{x}_i^t$  is the feature of node  $i$  in  $t$ -th time step,  $\mathbf{W}$  is trainable weights,  $\mathcal{N}(i)$  is the adjacent nodes of node  $i$ ,  $\mathbf{e}_{i,j}$  is the feature of edge between node  $i$  and  $j$ . MLP is multi-layer perceptron.

The update function used to update node features is Gated Recurrent Unit (GRU)<sup>25</sup>, as described by Supplementary Equation (7)

$$\mathbf{h}_i^t = \text{GRU}(\mathbf{h}_i^{t-1}, \mathbf{x}_i^t) \quad (6)$$

Where  $\mathbf{h}_i^t$  is the hidden state of node  $i$  in  $t$ -th time step.

For the readout phase, a feature vector for the whole graph is computed by enn-s2s that is based on iterative content-based attention from Vinyals et al<sup>26</sup> (Supplementary Equation 8-11)

$$\mathbf{q}_t = \text{LSTM}(\mathbf{q}_{t-1}^*) \quad (7)$$

$$\alpha_{i,t} = \frac{\exp(\mathbf{x}_i \cdot \mathbf{q}_t)}{\sum_{j \in \mathcal{G}} \exp(\mathbf{x}_j \cdot \mathbf{q}_t)} \quad (8)$$

$$\mathbf{r}_t = \sum_{i=1}^N \alpha_{i,t} \mathbf{x}_i \quad (9)$$

$$\mathbf{q}_t^* = \mathbf{q}_t \parallel \mathbf{r}_t \quad (10)$$

where  $i$  indexes through each node feature vector  $\mathbf{x}_i$ ,  $\mathbf{q}_t$  is a query vector which allows us to read  $\mathbf{r}_t$  from the memories at  $t$ -th time step,  $\alpha_{i,t}$  is attention coefficient of node  $i$  at  $t$ -th time step, and LSTM is Long Short-Term Memory<sup>27</sup> which calculates a recurrent state.  $\mathcal{G}$  is the graph to which node  $i$  and  $j$  belong.  $N$  is the number of nodes in graph  $\mathcal{G}$ .  $\parallel$  is concatenation.  $t$  is the step index, which is the number of times that the state is computed. enn-s2s is implemented by Pytorch Geometric<sup>28</sup>.

GCN was developed by Devogelaer et al for cocrystal screening<sup>19</sup> and its algorithm was mainly derived from Refs.<sup>29</sup> and<sup>30</sup>. The graph convolution operator of GCN trains a distinct weight matrix for each possible vertex degree, as shown in Supplementary Equation (11).

$$\mathbf{x}'_i = \mathbf{W}_1^{(\text{deg}(i))} \mathbf{x}_i + \mathbf{W}_2^{(\text{deg}(i))} \sum_{j \in \mathcal{N}(i)} \mathbf{x}_j \quad (11)$$

where  $\text{deg}(i)$  is the degree of node  $i$ .  $\mathbf{W}_1^{(\text{deg}(i))}$  and  $\mathbf{W}_2^{(\text{deg}(i))}$  are the trainable

weights for the node with degree  $\text{deg}(i)$ .  $\mathbf{x}_i$  is the feature vector of node  $i$ .  $\mathcal{N}(i)$  is the neighborhoods of node  $i$ .  $\mathbf{x}_j$  is the feature vectors of neighborhoods of node  $i$ . Following the GCN framework described in the work<sup>19</sup> (see Ref.<sup>19</sup> for more details), we build GCN by using DeepChem, and TensorFlow<sup>20</sup> is used for the backend.

**Bayesian optimization** is a sequential design strategy<sup>31</sup>, which is usually employed to optimize hyper-parameters of ML models<sup>19,32</sup>. Thus, we, in the work, also use it to search the optimal hyper-parameters of all the models, based on our cocrystal dataset. Concretely, we randomly split cross-validation set into a training (90%) and validation (10%) set. The value of the loss function as the objective of Bayesian optimizer. In each iteration, the model is trained for 100 epochs and the optimizer optimizes the hyperparameters of model for the next iteration based on the current hyperparameters and minimum loss in the validation set. In this work, we set the number of iterations as 100. After the 100 iterations, Bayesian optimizer will give the optimal hyperparameters. Supplementary Tables 2-3 list the searching space of hyperparameters for CCGNet, Graph-CNN, enn-s2s, SVM, RF and DNN-desc. The searching spaces of DNN-FP and GCN are adopted from Devogelaer's work<sup>19</sup>, thus not repeatedly listing them (see Ref.<sup>19</sup> for details). The best configuration of each model is shown in Supplementary Figure 5. Herein, Bayesian optimization is implemented by Python package Hyperopt<sup>33</sup>.

## **Construction of energetic cocrystal (ECC) dataset**

In order to finetune CCGNet model trained on the CC dataset to perform the transfer learning strategy, a training set composed of 243 energetic co-crystals is constructed (called as ECC dataset below), of which 116 positive samples are collected from CSD (Supplementary Table 11). Unfortunately, there are currently no public reports on failed experiments about the energetic cocrystals. Thus, we constructed the negative samples based on experimental experiences and a calculation criterion. In general, energetic molecules with strong rigidity and large steric hindrance are found to be difficult to interact with heterogeneous molecules. In addition, due to the competitive mechanism



of co-crystallization, molecules that have strong potential of homogeneous H-bonding tend to form single crystal will disfavor the formation of cocrystal between heterogeneous molecules<sup>34,35</sup>. Therefore, we select nine energetic molecules with these characteristics as cofomers of potential negative samples for the energetic cocrystals, as shown in Supplementary Figure 7(a). We combine the nine molecules with the cofomers from the positive samples of the energetic cocrystals, and initially yield 864 possible negative-samples of the energetic cocrystals. To further reduce the probability of the false negatives, we use the intermolecular site pairing energy (ISPE) proposed by Hunter et al.<sup>36</sup> as a screening criterion, which is based on the gas phase molecular electrostatic potential surfaces (MEPS) of each cofomer to calculate the intermolecular interaction energy, as reflected by Supplementary Equation (12):

$$\Delta E = E_{cc} - nE_1 - mE_2 \quad (12)$$

where  $E_1$  and  $E_2$  are ISPE values of conformer 1 and conformer 2, respectively.  $E_{cc}$  is ISPE of the cocrystal with stoichiometry ratio of  $n:m$  (1:1 in this work). The smaller the  $\Delta E$ , the higher the probability of co-crystallization. All cofomers are optimized at the level of B3LYP/6-31G (using Gaussian 09<sup>37</sup>) while MPES is calculated by Multiwfn<sup>38</sup>. The threshold of  $\Delta E$  is set to be -11 kJ/mol that was adopted from Hunter et al.<sup>36</sup>. Supplementary Table 12 shows ISPEs of the 864 negative samples, 815 of which satisfy  $\Delta E > -11$  kJ/mol. Considering the fact that the negative samples are combined by the computation method and only 116 positive samples from CSD in the training set of the energetic co-crystals, we randomly selected 118 negative samples from the 815 computational combinations into the training set. In addition, we also add nine negative samples from fifteen failed experiments in the co-crystallization with CL-20 in our laboratory to the training set, as shown in Supplementary Figure 7(b), and the remaining six failed combination pairs are selected into the independent set. Consequently, the ECC dataset that are used to finetune CCGNet contains 116 positive samples and 127 negative ones.

## Calculations of the impact sensitivity and heat of explosion to select the conformer of CL-20 for experimental synthesis

**Impact sensitivity (IS)** of energetic materials (EMs) is often evaluated by  $h_{50}$  that is a height of 50% probably in causing an explosion. Therefore, The higher  $h_{50}$ , the lower impact sensitivity. In this work, we used the empirical formula from Keshavarz<sup>39</sup> to evaluate  $h_{50}$  (Supplementary Equation 13).

$$\log(h_{50}) = \frac{52.13a + 31.80b + 117.6 \sum SSP_i}{MW} \quad (13)$$

Where  $a$  and  $b$  are the number of C and H atoms, respectively. The  $SSP_i$  is the specific structural parameters that can decrease or increase impact sensitivity. It can be specifically calculated according to molecular structures as: 1) The existence of amino derivatives as substituents in central heteroarene; 2) Attaching an aromatic ring (e.g. picryl) to nitrogen and presence of one nitro group in specific position; 3) The attachment of an aromatic ring to nitrogen in position 1 of nitro-1,2,3-triazole explosives. However, if one of substituents in polynitroheteroarenes contains another more active site for initiation of decomposition, e.g. R-NO<sub>2</sub>, the value of  $\sum SSP_i$  can be taken as zero. (see ref<sup>39</sup> for more details).

**The heat of explosion (Q)** refers to the total amount of energy released in the explosive reaction and is of great significance for gauging the explosion performance of the energetic compounds. Here Kamlet–Jacobs equations<sup>40</sup> are used to compute the heat of explosion  $Q$  (cal/g). For the energetic compound  $C_aH_bO_cN_d$ ,  $Q$  can be expressed by Supplementary Equations 14-16:

$$Q = \frac{28.9b + 94.05a + 0.239\Delta H_{298K}}{M} \quad \left( \text{if } c > 2a + \frac{b}{2} \right) \quad (14)$$

$$Q = \frac{28.9b + 94.05 \left( \frac{c}{2} - \frac{b}{4} \right) + 0.239\Delta H_{298K}}{M} \quad \left( \text{if } \frac{b}{2} < c < 2a + \frac{b}{2} \right) \quad (15)$$

$$Q = \frac{57.8c + 0.239\Delta H_{298K}}{M} \quad \left( \text{if } c < 2a + \frac{b}{2} \right) \quad (16)$$

where  $M$  is the molecular mass (g/mol) of  $C_aH_bO_cN_d$ .  $\Delta H_{298K}$  is the heat of formation derived from the atomization energy method that breaks down molecules into atoms and uses known isolated atoms to calculate the heat of formation and CBS-4M

electronic enthalpies<sup>41-44</sup>. The CBS-4M electronic enthalpies are calculated by using the Gaussian 09 program<sup>37</sup>. The heat of formation (kJ/mol) can be calculated by the atomization energy method, as expressed by Supplementary Equation 17:

$$\Delta H_{298K} = H_{(\text{molecule},298)} - \sum H_{(\text{atoms},298)}^{\circ} + \sum \Delta H_{f(\text{atoms},298)}^{\circ} \quad (17)$$

$H_{(\text{molecule},298)}$  denotes the calculated value of the heat of formation of molecules at 298K.  $H_{(\text{atoms},298)}^{\circ}$  is the sum of calculated heat of formation over all atoms at 298K while  $\Delta H_{f(\text{atoms},298)}^{\circ}$  is the sum of the experimental values of standard heat of formation over all atoms at 298K. Supplementary Table 14 lists the heat of formation values of the H, C, O and N atoms, derived from CBS-4M calculations and experiments<sup>17</sup>.

Supplementary Table 15 lists the impact sensitivity and the heat of explosion for the cofomers **5**, **7**, **8** and **10**. Due to the high sensitivity of CL-20, we tend to choose the cofomer with the relatively low sensitivity. The higher IS, the lower sensitivity. For the four cofomers, the sensitivities of the cofomers **8** and **10** are lower than those of the cofomers **5** and **7**. Despite the lowest sensitivity for the conformer **10**, its explosion heat  $Q$  calculated is also the lowest ( $0.797 \times 10^3 \text{ cal/g}$ ), which may disfavor the explosion performance of the cocrystal explosive. Compared to the cofomer **10**, the cofomer **8** has a higher explosive heat  $Q$  ( $1.174 \times 10^3 \text{ cal/g}$ ). Thus, trading off the impact sensitivity and the heat of explosion, we finally select the conformer **8** to make an attempt to synthesize its cocrystal with CL-20.

## **Energetic cocrystal synthesis and characterization**

**Material preparation.** 2,4,6,8,10,12-hexanitrohexaazaisowurtzitane ( $\epsilon$ -CL-20) was provided by the China Academy of Engineering Physics (CAEP). The 1-Methyl-4-nitropyrazole and other reagents used in this study were purchased online without further purification.

**Synthesis.** The raw materials  $\epsilon$ -CL-20 (438 mg, 1 mmol) and 1-Methyl-4-nitropyrazole

(127 mg, 1 mmol) were put into a round-bottom flask with anhydrous methanol (100mL) at room temperature. Then a magnetic stirring was used to stir the mixed solution until all the solids dissolve completely. The solution was filtered into a glass bottle which was sealed with a perforated seal film. Then solvent was evaporated at room temperature. After several days, CL-20/1-Methyl-4-nitropyrazole cocrystal was obtained.

**Single Crystal X-ray Diffraction (SXRD).** Single crystal Xray diffraction data for the cocrystal were collected using a Bruker APEX-II-CCD diffractometer with graphite-monochromated Mo-K $\alpha$  radiation ( $\lambda = 0.71073 \text{ \AA}$ ). The crystal was kept at 296 K during data collection. The data were processed using Olex2 software. The structures were solved and refined with SHELXL. All non-hydrogen atoms were refined anisotropically, and hydrogen atoms were refined using the riding mode. A high quality cocrystal of CL-20/1-Methyl-4-nitropyrazole was characterized by SXRD. The crystallographic data for the cocrystal are illustrated in Supplementary Table 16. The crystal structure is shown in Supplementary Figure 8(a)-(b). Supplementary Figure 8(a) is ORTEP plot of the cocrystal. The CL-20 molecules and 1-Methyl-4-nitropyrazole molecules stack together in a sandwich-like style shown in Supplementary Figure 8(b).

## Supplementary References

- 1 Veronika, S., Ondřej, D., Gregor, S., Eliška, S. & Bohumil, K. Ivabradine Hydrochloride (S)-Mandelic Acid Co-Crystal: In Situ Preparation during Formulation. *Crystals* **7**, 13 (2017).
- 2 Yamamoto, K., Tsutsumi, S. & Ikeda, Y. Establishment of cocrystal cocktail grinding method for rational screening of pharmaceutical cocrystals. *International Journal of Pharmaceutics* **437**, 162-171, doi:<https://doi.org/10.1016/j.ijpharm.2012.07.038> (2012).
- 3 Félix-Sonda, B. C., Rivera-Islas, J., Herrera-Ruiz, D., Morales-Rojas, H. & Höpfl, H. Nitazoxanide Cocrystals in Combination with Succinic, Glutaric, and 2,5-Dihydroxybenzoic Acid. *Crystal Growth & Design* **14**, 1086-1102, doi:10.1021/cg4015916 (2014).
- 4 Kant, V. Study of phase diagram and microstructures of some nicotinamide based binary organic eutectic. *Bulletin of Pharmaceutical and Medical Sciences (BOPAMS)* **1** (2013).
- 5 Wu, T.-k., Lin, S.-Y., Lin, H.-L. & Huang, Y.-T. Simultaneous DSC-FTIR microspectroscopy used to screen and detect the co-crystal formation in real time. *Bioorganic & Medicinal Chemistry Letters* **21**, 3148-3151, doi:<https://doi.org/10.1016/j.bmcl.2011.03.001> (2011).
- 6 Wicker, J. G. *et al.* Will they co-crystallize? *CrystEngComm* **19**, 5336-5340 (2017).
- 7 Kant, V. Nicotinamide–Indole Binary Drug System: Thermodynamic and Interfacial Studies. *Molecular Crystals and Liquid Crystals* **608**, 211-222 (2015).
- 8 Childs, S. L. *et al.* Screening strategies based on solubility and solution composition generate pharmaceutically acceptable cocrystals of carbamazepine. *CrystEngComm* **10**, 856-864, doi:10.1039/B715396A (2008).
- 9 Habgood, M., Deij, M. A., Mazurek, J., Price, S. L. & ter Horst, J. H. Carbamazepine Co-crystallization with Pyridine Carboxamides: Rationalization by Complementary Phase Diagrams and Crystal Energy Landscapes. *Crystal Growth & Design* **10**, 903-912, doi:10.1021/cg901230b (2010).
- 10 Mohammad, M. A., Alhalaweh, A. & Velaga, S. P. Hansen solubility parameter as a tool to predict cocrystal formation. *International Journal of Pharmaceutics* **407**, 63-71, doi:<https://doi.org/10.1016/j.ijpharm.2011.01.030> (2011).
- 11 Wood, P. A. *et al.* Knowledge-based approaches to co-crystal design. *CrystEngComm* **16**, 5839-5848, doi:10.1039/C4CE00316K (2014).
- 12 Klímová, K. & Leitner, J. DSC study and phase diagrams calculation of binary systems of paracetamol. *Thermochimica Acta* **550**, 59-64, doi:<https://doi.org/10.1016/j.tca.2012.09.024> (2012).
- 13 Karki, S. *et al.* Improving Mechanical Properties of Crystalline Solids by

- Cocrystal Formation: New Compressible Forms of Paracetamol. *Advanced Materials* **21**, 3905-3909, doi:<https://doi.org/10.1002/adma.200900533> (2009).
- 14 Berry, D. J. *et al.* Applying Hot-Stage Microscopy to Co-Crystal Screening: A Study of Nicotinamide with Seven Active Pharmaceutical Ingredients. *Crystal Growth & Design* **8**, 1697-1712, doi:10.1021/cg800035w (2008).
- 15 Szczepanik, R. Two- and multicomponent, solid-liquid systems formed by aromatic hydrocarbons, anthraquinone, and coal-tar fractions. *Chem. Stosowana Ser. A* **7**, 621-660 (1963).
- 16 Rice, J. W. & Suuberg, E. M. Thermodynamic study of (anthracene+benzo[a]pyrene) solid mixtures. *The Journal of Chemical Thermodynamics* **42**, 1356-1360, doi:<https://doi.org/10.1016/j.jct.2010.05.019> (2010).
- 17 Linstrom, P. & Mallard, W. (National Institute of Standards and Technology (Gaithersburg, MD 20899), 2003).
- 18 Swami, A. & Jain, R. Scikit-learn: Machine Learning in Python. *Journal of Machine Learning Research* **12**, 2825-2830 (2013).
- 19 Devogelaer, J.-J., Meekes, H., Tinnemans, P., Vlieg, E. & de Gelder, R. Co-crystal Prediction by Artificial Neural Networks\*\*. *Angewandte Chemie International Edition* **59**, 21711-21718, doi:<https://doi.org/10.1002/anie.202009467> (2020).
- 20 Abadi, M. *et al.* *TensorFlow: A system for large-scale machine learning.* (2016).
- 21 Such, F. P. *et al.* Robust Spatial Filtering With Graph Convolutional Neural Networks. *IEEE J. Sel. Top. Signal Process.* **11**, 884-896, doi:10.1109/jstsp.2017.2726981 (2017).
- 22 Ioffe, S. & Szegedy, C. Batch Normalization: Accelerating Deep Network Training by Reducing Internal Covariate Shift. (2015).
- 23 Battaglia, P. W. *et al.* Relational inductive biases, deep learning, and graph networks. *arXiv preprint arXiv:1806.01261* (2018).
- 24 Gilmer, J., Schoenholz, S. S., Riley, P. F., Vinyals, O. & Dahl, G. E. Neural message passing for quantum chemistry. *arXiv preprint arXiv:1704.01212* (2017).
- 25 Cho, K., Van Merriënboer, B., Bahdanau, D. & Bengio, Y. On the Properties of Neural Machine Translation: Encoder-Decoder Approaches. *Computer ence* (2014).
- 26 Vinyals, O., Bengio, S. & Kudlur, M. Order Matters: Sequence to sequence for sets. *Computer ence* (2015).
- 27 Hochreiter, S. & Schmidhuber, J. Long Short-Term Memory. *Neural Computation* **9**, 1735-1780 (1997).
- 28 Fey, M. & Lenssen, J. E. Fast graph representation learning with PyTorch Geometric. *arXiv preprint arXiv:1903.02428* (2019).
- 29 Duvenaud, D. *et al.* in *NIPS*.
- 30 Altae-Tran, H., Ramsundar, B., Pappu, A. S. & Pande, V. Low Data Drug Discovery with One-Shot Learning. *ACS Central Science* **3**, 283-293,

- doi:10.1021/acscentsci.6b00367 (2017).
- 31 Shahriari, B., Swersky, K., Wang, Z., Adams, R. P. & Freitas, N. d. Taking the Human Out of the Loop: A Review of Bayesian Optimization. *Proceedings of the IEEE* **104**, 148-175, doi:10.1109/JPROC.2015.2494218 (2016).
- 32 Stokes, J. M. *et al.* A Deep Learning Approach to Antibiotic Discovery. *Cell* **181**, 475-483, doi:<https://doi.org/10.1016/j.cell.2020.04.001> (2020).
- 33 Bergstra, J., Yamins, D. & Cox, D. D. Making a science of model search. *arXiv preprint arXiv:1209.5111* (2012).
- 34 Ross, S., Lamprou, D. & Douroumis, D. Engineering and manufacturing of pharmaceutical co-crystals: a review of solvent-free manufacturing technologies. *Chemical Communications* **52**, 8772-8786 (2016).
- 35 Etter, M. C. & Reutzel, S. M. Hydrogen bond directed cocrystallization and molecular recognition properties of acyclic imides. *Journal of the American Chemical Society* **113**, 2586-2598, doi:10.1021/ja00007a037 (1991).
- 36 Musumeci, D., Hunter, C. A., Prohens, R., Scuderi, S. & McCabe, J. F. Virtual cocrystal screening. *Chemical Science* **2**, 883-890 (2011).
- 37 Gaussian 09, Revision B.01 (Wallingford, CT, 2009).
- 38 Lu, T. & Chen, F. Multiwfn: A multifunctional wavefunction analyzer. *Journal of Computational Chemistry* **33**, 580-592, doi:<https://doi.org/10.1002/jcc.22885> (2012).
- 39 Keshavarz, M. H., Zali, A. & Shokrolahi, A. A simple approach for predicting impact sensitivity of polynitroheteroarenes. *Journal of Hazardous Materials* **166**, 1115-1119, doi:<https://doi.org/10.1016/j.jhazmat.2008.12.022> (2009).
- 40 Kamlet, M. J. & Jacobs, S. J. Chemistry of Detonations. I. A Simple Method for Calculating Detonation Properties of C–H–N–O Explosives. *The Journal of Chemical Physics* **48**, 23-35, doi:10.1063/1.1667908 (1968).
- 41 Fischer, D., Klapötke, T. M., Reymann, M. & Stierstorfer, J. Dense Energetic Nitraminofurazanes. *Chemistry – A European Journal* **20**, 6401-6411, doi:<https://doi.org/10.1002/chem.201400362> (2014).
- 42 Curtiss, L. A., Raghavachari, K., Redfern, P. C. & Pople, J. A. Assessment of Gaussian-2 and density functional theories for the computation of enthalpies of formation. *The Journal of Chemical Physics* **106**, 1063-1079, doi:10.1063/1.473182 (1997).
- 43 Göbel, M., Karaghiosoff, K., Klapötke, T. M., Piercey, D. G. & Stierstorfer, J. Nitrotetrazolate-2N-oxides and the Strategy of N-Oxide Introduction. *Journal of the American Chemical Society* **132**, 17216-17226, doi:10.1021/ja106892a (2010).
- 44 Xie, Y. *et al.* A property-oriented adaptive design framework for rapid discovery of energetic molecules based on small-scale labeled datasets. *RSC Advances* **11**, 25764-25776, doi:10.1039/D1RA03715C (2021).